Hand-In #3

Continuous Time Finance 2 (FinKont2)

Youssef Raad (zfw568)

April 14, 2024

"Dying For The Right Cause. It's The Most Human Thing We Can Do."

Contents

†Note†

I have completed the handin assignment as per the instructions provided in the assignment description. However, I encountered an issue where certain questions appear to be missing:

- Showing respective conditions for E_j is **left in** as it is removed in the latest version but no notice was given (Subsection 1.2).
- Showing the solutions of ODE's equation (29) and (30) are given by equation (31) and (32), respectively, are **left out** since notice was given (Subsection 3.2).

1 Characteristic functions in the Heston model

The single digit referencing to equation (x) is for equations in the HandIn #3 description. If equations are refered within this document we will use a double digit referencing (x.y) where x is the section number and y the equation number.

1.1 Changing variables and guessing the form of solution

⋆ Let $\Psi_j := \Psi^j_{x(T)}(x, v, t; u)$, $j = 1, 2$ and $\tau = T - t$. Let the reparametrization of Ψ_j through $\tau = T - t$ be given by $\Psi^j_{x(T)}(x, v, \tau; u)$. The transformations of terms in equation (4) is then given by noticing only the first term depends on τ:

$$\begin{aligned}
\frac{\partial}{\partial t}\Psi^j_{x(T)}(x, v, t; u) &= -\frac{\partial}{\partial \tau}\Psi^j_{x(T)}(x, v, \tau; u),\\
\frac{\partial}{\partial x}\Psi^j_{x(T)}(x, v, t; u) &= \frac{\partial}{\partial x}\Psi^j_{x(T)}(x, v, \tau; u),\\
\frac{\partial^2}{\partial x^2}\Psi^j_{x(T)}(x, v, t; u) &= \frac{\partial^2}{\partial x^2}\Psi^j_{x(T)}(x, v, \tau; u),\\
\frac{\partial}{\partial v}\Psi^j_{x(T)}(x, v, t; u) &= \frac{\partial}{\partial v}\Psi^j_{x(T)}(x, v, \tau; u),\\
\frac{\partial^2}{\partial v^2}\Psi^j_{x(T)}(x, v, t; u) &= \frac{\partial^2}{\partial v^2}\Psi^j_{x(T)}(x, v, \tau; u),\\
\frac{\partial^2}{\partial v \partial x}\Psi^j_{x(T)}(x, v, t; u) &= \frac{\partial^2}{\partial v \partial x}\Psi^j_{x(T)}(x, v, \tau; u).
\end{aligned}$$

As the only transformation that differs from equation (4) through the reparametrization is the first, namely:

$$\frac{\partial}{\partial t}\Psi_j = -\frac{\partial}{\partial \tau}\Psi^j_{x(T)}(x, v, \tau; u),$$

we achieve equation (6) from substitution of the differing term into equation (4) using the shorhand notation:

$$0 = -\frac{\partial \Psi_j}{\partial \tau} + (r + u_j v)\frac{\partial \Psi_j}{\partial x} + \frac{1}{2}v\frac{\partial^2 \Psi_j}{\partial x^2} + \rho\sigma v\frac{\partial^2 \Psi_j}{\partial v \partial x} + \frac{1}{2}\sigma^2 v\frac{\partial^2 \Psi_j}{\partial v^2} + (a - b_j v)\frac{\partial \Psi_j}{\partial v},$$

as desired.

The terminal condition follows simply from observering that at $t = T$ we have $\tau = T - t = T - T = 0$. Hence, through the reparametrization using τ we achieve equation (7):

$$e^{iux} = \Psi^j_{x(T)}(x, v, 0; u) \quad \forall (x, v) \in \mathbb{R} \times (0, +\infty),$$

as desired.

⋆ Equation (8) is given by:

$$\Psi^j_{x(T)}(x,v,t;u) = \exp\left\{C_j(\tau;u) + D_j(\tau;u)v + iux\right\}.$$

We substitute in the ansatz (the guessed solution) (8) into equation (6) and equation (7) using the shorthands $C_j(\tau;u) := C_j$ and $D_j(\tau;u) = D_j$ yielding the PDE:

$$\begin{aligned}
0 &= -\frac{\partial\Psi_j}{\partial\tau} + (r+u_jv)\frac{\partial\Psi_j}{\partial x} + \frac{1}{2}v\frac{\partial^2\Psi_j}{\partial x^2} + \rho\sigma v\frac{\partial^2\Psi_j}{\partial v\partial x} + \frac{1}{2}\sigma^2 v\frac{\partial^2\Psi_j}{\partial v^2} + (a-b_jv)\frac{\partial\Psi_j}{\partial v} \\
&\overset{\dagger}{=} -\left(\frac{\partial C_j}{\partial\tau} + \frac{\partial D_j}{\partial\tau}v\right)\Psi_j + (r+u_jv)(iu)\Psi_j \\
&\quad + \frac{1}{2}(iu)^2\Psi_j + \rho\sigma v(D_j)(iu)\Psi_j + \frac{1}{2}\sigma^2 v(D_j)^2\Psi_j + (a-b_jv)(D_j)\Psi_j \\
&\overset{\dagger\dagger}{=} \Psi_j\left\{\underbrace{-\frac{\partial C_j}{\partial\tau} + aD_j + rui}_{(*)}\right\} + \Psi_j v\left\{\underbrace{-\frac{\partial D_j}{\partial\tau} + u_jui - \frac{1}{2}u^2 + \rho\sigma uiD_j + \frac{1}{2}\sigma^2D_j^2 - b_jD_j}_{(**)}\right\},
\end{aligned}$$

where † follows from differentiation and †† from the fact that $i^2 = (\sqrt{-1})^2 = -1$ and thus $(iu)^2 = (-1)\cdot u^2 = -u^2$.

1.2 Transforming the PDE to a system of ODEs and solving it

⋆ The PDE that we derived in Subsection 1.1 is satisfied if and only if both ordinary differential equations $(*)$ and $(**)$ equal 0 for all $(x,v) \in \mathbb{R}\times(0,\infty)$. Consequently, the two ordinary differential equations from $(*)$ and $(**)$ can be solved seperately. i.e a system of two ODE's. The system of two ordinary differential equations is then found by dropping Ψ_j-terms, rewriting and thus given by $(*)$:

$$\begin{aligned}
0 &= -\frac{\partial C_j}{\partial\tau} + aD_j + rui \\
&\iff \\
\frac{\partial C_j}{\partial\tau} &= aD_j + rui,
\end{aligned}$$

and $(**)$:

$$\begin{aligned}
0 &= -\frac{\partial D_j}{\partial\tau} + u_jui - \frac{1}{2}u^2 + \rho\sigma uiD_j + \frac{1}{2}\sigma^2D_j^2 - b_jD_j \\
&\iff \\
\frac{\partial D_j}{\partial\tau} &= u_jui - \frac{1}{2}u^2 + \rho\sigma uiD_j + \frac{1}{2}\sigma^2D_j^2 - b_jD_j.
\end{aligned}$$

At $\tau = 0$, the initial conditions are zero-initial conditions, i.e such that $D_j(0;u) = 0$ and $C_j(0;u) = 0$. This is because when the expiry is reached ($\tau = 0$), the value of $x_T = \log S_T$ is established, eliminating the expectation in the equality:

$$\begin{aligned}
\Psi_j &:= \mathbb{E}^{\mathbb{P}_j}\left[e^{iux} \mid x(t) = x, v(t) = v\right] \\
&= \exp\left\{C_j(\tau;u) + D_j(\tau;u)\cdot v + iux\right\} \quad j = 1,2.
\end{aligned}$$

As a result, the second equality has to simplifiy to e^{iux} as the expectation vanishes at $\tau = 0$:

$$\begin{aligned} \Psi^j_{x_{(T)}}(x, v, 0; u) &= e^{iux} \\ &\Rightarrow \\ \exp\{C_j(0; u) + D_j(0; u) \cdot v + iux\} &= e^{iux} \\ &\Longleftrightarrow \\ C_j(0; u) + D_j(0; u) \cdot v &= 0 \end{aligned}$$

This leads to the conclusion that the sufficient initial conditions at $\tau = 0$ are $D_j(0, u) = 0$ and $C_j(0, u) = 0$. The equation denoted by (**) outlines a Riccati equation in D_j that, importantly, does not depend on C_j, while the equation marked by (*) represents an ordinary differential equation for C_j. This ordinary differential equation can be readily solved through direct integration of D_j after determining D_j.

$\star$ We now proceed to solving the Riccati equation as of the beforementioned reasons, i.e that it contains terms involving only the functions D_j and not C_j. We have that:

$$\begin{aligned} \frac{\partial D_j}{\partial \tau} &= u_j ui - \frac{1}{2}u^2 + \rho\sigma ui D_j + \frac{1}{2}\sigma^2 D_j^2 - b_j D_j \\ &= u_j ui - \frac{1}{2}u^2 - (b_j - \rho\sigma ui)D_j + \frac{\sigma^2}{2}D_j^2 \\ &= \alpha - \beta D_j + \frac{1}{2}\sigma^2 D_j^2, \end{aligned}$$

with:

$$\alpha = u_j ui - \frac{1}{2}u^2 \quad \text{and} \quad \beta = b_j - \rho\sigma ui.$$

The solution given in (9) can then be written exactly as:

$$D_j(\tau; u) = -\frac{\frac{\partial E_j(\tau;u)}{\partial \tau}}{\frac{1}{2}\sigma^2 E_j(\tau; u)}.$$

If we now differentiate the RHS of (9) wrt. τ we achieve:

$$\begin{aligned} \frac{\partial D_j}{\partial \tau} &= -\frac{\frac{\partial^2 E_j}{\partial \tau^2} E_j \frac{1}{2}\sigma^2 - \left(\frac{\partial E_j}{\partial \tau}\right)^2 \frac{1}{2}\sigma^2}{\left(\frac{1}{2}\sigma^2 E_j\right)^2} \\ &= \frac{\left(\frac{\partial E_j}{\partial \tau}\right)^2 - \frac{\partial^2 E_j}{\partial \tau^2} E_j}{\frac{1}{2}\sigma^2 E_j^2}. \end{aligned}$$

Substituting (9) and its just found derivatives into the Ricatti equation yields:

$$\begin{aligned}
\frac{\partial D_j}{\partial \tau} &= \alpha - \beta D_j + \frac{1}{2}\sigma^2 D_j^2 \\
&\iff \\
\frac{\left(\frac{\partial E_j}{\partial \tau}\right)^2 - \frac{\partial^2 E_j}{\partial \tau^2} E_j}{\frac{1}{2}\sigma^2 E_j^2} &= \alpha - \beta \frac{-\frac{\partial E_j D}{\partial \tau}}{\frac{1}{2}\sigma^2 E_j} + \frac{1}{2}\sigma^2 \left(\frac{-\frac{\partial E_j}{\partial \tau}}{\frac{1}{2}\sigma^2 E_j}\right)^2 \\
&\iff \\
\frac{\left(\frac{\partial E_j}{\partial \tau}\right)^2 - \frac{\partial^2 E_j}{\partial \tau^2} E_j}{\frac{1}{2}\sigma^2 E_j^2} &= \alpha + \beta \frac{\frac{\partial E_j D}{\partial \tau}}{\frac{1}{2}\sigma^2 E_j} + \frac{\left(\frac{\partial E_j}{\partial \tau}\right)^2}{\frac{1}{2}\sigma^2 E_j} \\
&\iff \\
\left(\frac{\partial E_j}{\partial \tau}\right)^2 - \frac{\partial^2 E_j}{\partial \tau^2} &= \alpha \frac{1}{2}\sigma^2 E_j^2 + \beta \frac{\frac{\partial E_j}{\partial \tau}}{\frac{1}{2}\sigma^2 E_j} \frac{1}{2}\sigma^2 E_j^2 + \frac{\left(\frac{\partial E_j}{\partial \tau}\right)^2}{\frac{1}{2}\sigma^2 E_j} \frac{1}{2}\sigma^2 E_j^2 \\
&\iff \\
\left(\frac{\partial E_j}{\partial \tau}\right)^2 - \frac{\partial^2 E_j}{\partial \tau^2} &= \alpha \frac{1}{2}\sigma^2 E_j^2 + \beta \frac{\partial E_j}{\partial \tau} E_j + \left(\frac{\partial E_j}{\partial \tau}\right)^2 \\
&\iff \\
-\frac{\partial^2 E_j}{\partial \tau^2} E_j &= \alpha \frac{1}{2}\sigma^2 E_j^2 + \beta \frac{\partial E_j}{\partial \tau} E_j \\
&\iff \\
-\frac{\partial^2 E_j}{\partial \tau^2} &= \alpha \frac{1}{2}\sigma^2 E_j + \beta \frac{\partial E_j}{\partial \tau} \\
&\iff \\
\frac{\partial^2 E_j}{\partial \tau^2} + \alpha \frac{1}{2}\sigma^2 E_j + \beta \frac{\partial E_j}{\partial \tau} &= 0 \\
&\overset{\dagger}{\iff} \\
\frac{\partial^2 E_j}{\partial \tau^2} - (\rho u \sigma i - b_j)\frac{\partial E_j}{\partial \tau} + \frac{\sigma^2}{2}\left(-\frac{1}{2}u^2 + u_j u i\right) E_j &= 0,
\end{aligned}$$

where † follows from $\alpha = u_j u i - \frac{1}{2}u^2$ and $\beta = b_j - \rho\sigma u i$ and rearranging.

⋆ We showed the initial sufficient condition for $\tau = 0$ was specified as $D_j(0;u) = 0$. We exploit this to show that the respective sufficient conditions for E_j are given by:

$$\begin{aligned}
D_j(0;u) = -\frac{\frac{\partial E_j(\tau;u)}{\partial \tau}\Big|_{\tau=0}}{\frac{1}{2}\sigma^2 E_j(0;u)} &= 0 \\
&\iff \\
\frac{\partial E_j(\tau;u)}{\partial \tau}\Big|_{\tau=0} &= 0.
\end{aligned}$$

Using this result and that we just showed the resulting ODE for E_j we now have that:

$$\left(\frac{\partial^2 E_j(\tau;u)}{\partial\tau^2}\bigg|_{\tau=0}\right) - (\rho u\sigma i - b_j)\underbrace{\left(\frac{\partial E_j(\tau;u)}{\partial\tau}\bigg|_{\tau=0}\right)}_{=0} + \frac{\sigma^2}{2}\left(-\frac{1}{2}u^2 + u_j ui\right)E_j(0;u) = 0$$

$$\iff$$

$$\left(\frac{\partial^2 E_j(\tau;u)}{\partial\tau^2}\bigg|_{\tau=0}\right) + \frac{\sigma^2}{2}\left(-\frac{1}{2}u^2 + u_j ui\right)E_j(0;u) = 0$$

$$\iff$$

$$-\frac{2}{\sigma^2}\frac{\frac{\partial^2 E_j(\tau;u)}{\partial\tau^2}\Big|_{\tau=0}}{\left(-\frac{1}{2}u^2 + u_j ui\right)} = E_j(0;u)$$

$$\neq 0,$$

yielding the respective sufficient condition for E_j at $\tau = 0$.

⋆ For $\tau = 0$, we achieve the following form of equation (10):

$$\begin{aligned} E_j(0;u) &= A_j e^{x_{j,+}\cdot 0} + B_j e^{x_{j,-}\cdot 0} \\ &= A_j \cdot 1 + B_j \cdot 1 \\ &= A_j + B_j, \end{aligned}$$

showing the first property.

We now find the derivative of equation (10) to find the initial condition of said derivative:

$$\frac{\partial E_j(\tau;u)}{\partial\tau} = x_{j,+}A_j e^{x_{j,+}\cdot\tau} + x_{j,-}B_j e^{x_{j,-}\cdot\tau}.$$

This now yields the sufficient initial condition of the derivative of E_j:

$$\begin{aligned} \frac{\partial E_j(\tau;u)}{\partial\tau}\bigg|_{\tau=0} &= x_{j,+}A_j e^{x_{j,+}\cdot 0} + x_{j,-}B_j e^{x_{j,-}\cdot 0} \\ &= x_{j,+}\cdot 1\cdot A_j + x_{j,-}\cdot 1\cdot B_j \\ &= x_{j,+}A_j + x_{j,-}B_j. \end{aligned}$$

⋆ Once again, we use the sufficient initial conditions for D_j, namely, $D_j(0;u) = 0$, for $\tau = 0$. For equation (9) to hold, it must then be the case that:

$$\frac{\partial E_j(\tau;u)}{\partial\tau}\bigg|_{\tau=0} = 0.$$

This gives us the bi-implications:

$$\begin{aligned} \frac{\partial E_j(\tau;u)}{\partial\tau}\bigg|_{\tau=0} &= 0 \\ &\iff \\ x_{j,+}A_j + x_{j,-}B_j &= 0 \\ &\overset{\dagger}{\iff} \end{aligned}$$

$$-A_j = \frac{x_{j,-}}{x_{j,+}}B_j = g_j B_j \quad \text{and} \quad B_j = \frac{x_{j,+}}{x_{j,-}}A_j = -g_j^{-1}A_j,$$

where † follows from definition, namely, $g_j = \frac{x_{j,-}}{x_{j,+}}$. Using our just showed result, $E_j(0;u) = A_j + B_j$, we find that:

$$\begin{aligned} -A_j = g_j B_j &= g_j(E_j(0;u) - A_j) \\ &\iff \\ A_j(g_j - 1) &= g_j E_j(0;u) \\ &\iff \\ A_j &= \frac{g_j E_j(0;u)}{g_j - 1}, \end{aligned}$$

implying by the found relations of A_j, B_j:

$$B_j = -g_j^{-1} A_j = -g_j^{-1} \frac{g_j E_j(0;u)}{g_j - 1} = -\frac{E_j(0;u)}{g_j - 1}.$$

⋆ It now follows quite simply and nicely from substitution of the previous results that:

$$\begin{aligned} E_j(\tau;u) &= A_j e^{x_{j,+}\cdot\tau} + B_j e^{x_{j,-}\cdot\tau} \\ &= \frac{g_j E_j(0;u)}{g_j - 1} e^{x_{j,+}\cdot\tau} - \frac{E_j(0;u)}{g_j - 1} e^{x_{j,-}\cdot\tau} \\ &= \frac{E_j(0;u)}{g_j - 1} \left(g_j e^{x_{j,+}\cdot\tau} - e^{x_{j,-}\cdot\tau} \right). \end{aligned}$$

⋆ We use the found relations for A_j, B_j to find:

$$\begin{aligned} \frac{\partial E_j(\tau;u)}{\partial \tau} &= x_{j,+} A_j e^{x_{j,+}\cdot\tau} + x_{j,-} B_j e^{x_{j,-}\cdot\tau} \\ &= x_{j,+} \frac{g_j E_j(0;u)}{g_j - 1} e^{x_{j,+}\tau} - x_{j,-} \frac{E_j(0;u)}{g_j - 1} e^{x_{j,-}\cdot\tau} \\ &= \frac{E_j(0;u)}{g_j - 1} \left(x_{j,+} g_j e^{x_{j,+}\cdot\tau} - x_{j,-} e^{x_{j,-}\cdot\tau} \right). \end{aligned}$$

⋆ Substituting E_j and $\partial E_j / \partial \tau$ into equation (9) for D_j now yields the altered expression:

$$\begin{aligned} D_j(\tau;u) &= -\frac{\frac{\partial E_j(\tau;u)}{\partial \tau}}{\frac{1}{2}\sigma^2 E_j(\tau;u)} \\ &= -\frac{\frac{E_j(0;u)}{g_j - 1} \left(x_{j,+} g_j e^{x_{j,+}\cdot\tau} - x_{j,-} e^{x_{j,-}\cdot\tau} \right)}{\frac{1}{2}\sigma^2 \frac{E_j(0;u)}{g_j - 1} \left(g_j e^{x_{j,+}\cdot\tau} - e^{x_{j,-}\cdot\tau} \right)} \end{aligned}$$

Now, substituting in equation (11) and (15) into the altered equation (9) using $\exp\{\}$ for readability yields:

$$
\begin{aligned}
D_j(\tau;u) &= -\frac{\frac{E_j(0;u)}{g_j-1}\left(x_{j,+}g_j\exp\{x_{j,+}\cdot\tau\}-x_{j,-}\exp\{x_{j,-}\cdot\tau\}\right)}{\frac{\sigma^2}{2}\frac{E_j(0;u)}{g_j-1}\left(g_j\exp\{x_{j,+}\cdot\tau\}-\exp\{x_{j,-}\cdot\tau\}\right)} \\
&= -\frac{\frac{E_j(0;u)}{g_j-1}\left(\frac{\rho\sigma ui-b_j+d_j}{2}g_j\exp\left\{\frac{\rho\sigma ui-b_j+d_j}{2}\tau\right\}-\frac{\rho\sigma ui-b_j-d_j}{2}\exp\left\{\frac{\rho\sigma ui-b_j-d_j}{2}\tau\right\}\right)}{\frac{\sigma^2}{2}\frac{E_j(0;u)}{g_j-1}\left(g_j\exp\left\{\frac{\rho\sigma ui-b_j+d_j}{2}\tau\right\}-\exp\left\{\frac{\rho\sigma ui-b_j-d_j}{2}\tau\right\}\right)} \\
&= -\frac{\frac{\rho\sigma ui-b_j+d_j}{2}g_j\exp\left\{\frac{\rho\sigma ui-b_j+d_j}{2}\tau\right\}-\frac{\rho\sigma ui-b_j-d_j}{2}\exp\left\{\frac{\rho\sigma ui-b_j-d_j}{2}\tau\right\}}{\frac{\sigma^2}{2}\left(g_j\exp\left\{\frac{\rho\sigma ui-b_j+d_j}{2}\tau\right\}-\exp\left\{\frac{\rho\sigma ui-b_j-d_j}{2}\tau\right\}\right)} \\
&= -\frac{\frac{\rho\sigma ui-b_j+d_j}{2}g_j\exp\left\{\frac{d_j}{2}\tau\right\}-\frac{\rho\sigma ui-b_j-d_j}{2}\exp\left\{-\frac{d_j}{2}\tau\right\}}{\frac{\sigma^2}{2}\left(g_j\exp\left\{\frac{d_j}{2}\tau\right\}-\exp\left\{-\frac{d_j}{2}\tau\right\}\right)} \\
&= -\frac{\left(\rho\sigma ui-b_j+d_j\right)g_j\exp\left\{\frac{d_j}{2}\tau\right\}-\left(\rho\sigma ui-b_j-d_j\right)\exp\left\{-\frac{d_j}{2}\tau\right\}}{\sigma^2\left(g_j\exp\left\{\frac{d_j}{2}\tau\right\}-\exp\left\{-\frac{d_j}{2}\tau\right\}\right)} \\
&\overset{\dagger}{=} -\frac{\left(\rho\sigma ui-b_j+d_j\right)g_j\exp\left\{\frac{d_j}{2}\tau\right\}\exp\left\{\frac{d_j}{2}\tau\right\}-\left(\rho\sigma ui-b_j-d_j\right)\exp\left\{-\frac{d_j}{2}\tau\right\}\exp\left\{\frac{d_j}{2}\tau\right\}}{\sigma^2\left(g_j\exp\left\{\frac{d_j}{2}\tau\right\}\exp\left\{\frac{d_j}{2}\tau\right\}-\exp\left\{-\frac{d_j}{2}\tau\right\}\exp\left\{\frac{d_j}{2}\tau\right\}\right)} \\
&= -\frac{\left(\rho\sigma ui-b_j+d_j\right)g_j\exp\{d_j\tau\}-\left(\rho\sigma ui-b_j-d_j\right)}{\sigma^2\left(g_j\exp\{d_j\tau\}-1\right)} \\
&\overset{\dagger\dagger}{=} -\frac{\left(\rho\sigma ui-b_j+d_j\right)\frac{\rho\sigma ui-b_j-d_j}{\rho\sigma ui-b_j+d_j}\exp\{d_j\tau\}-\left(\rho\sigma ui-b_j-d_j\right)}{\sigma^2\left(g_j\exp\{d_j\tau\}-1\right)} \\
&= -\frac{\left(\rho\sigma ui-b_j-d_j\right)\exp\{d_j\tau\}-\left(\rho\sigma ui-b_j-d_j\right)}{\sigma^2\left(g_j\exp\{d_j\tau\}-1\right)} \\
&\overset{\dagger\dagger\dagger}{=} -\frac{\left(b_j-\rho\sigma ui+d_j\right)\exp\{d_j\tau\}-\left(b_j-\rho\sigma ui+d_j\right)}{\sigma^2\left(1-g_j\exp\{d_j\tau\}\right)} \\
&= \frac{\left(b_j-\rho\sigma ui+d_j\right)\left(1-\exp\{d_j\tau\}\right)}{\sigma^2\left(1-g_j\exp\{d_j\tau\}\right)} \\
&= \frac{b_j-\rho\sigma ui+d_j}{\sigma^2}\frac{1-\exp\{d_j\tau\}}{1-g_j\exp\{d_j\tau\}},
\end{aligned}
$$

where $\dagger$ follows by multiplication of $\exp\left\{\frac{d_j}{2}\tau\right\}$, $\dagger\dagger$ from $g := x_{j,-}/x_{j,+}$ and $\dagger\dagger\dagger$ by multiplication of -1.

$\star$ As stated at the very start, finding the solution of D_j is advantageous to derive the solution for C_j as the ODE for C_j was given by $(*)$ containing D_j. So, by integration:

$$\begin{aligned}
\frac{\partial C_j}{\partial \tau} &= rui + aD_j \\
&\iff \\
C_j &= \int_0^\tau rui + aD_j(s;u)\, ds \\
&\overset{\dagger}{=} rui \int_0^\tau ds + a\int_0^\tau D_j(s;u)\, ds \\
&= rui\,(\tau - 0) + a\int_0^\tau D_j(s;u)\, ds \\
&= rui\tau + a\int_0^\tau D_j(s;u)\, ds.
\end{aligned}$$

where † follows from the linearity of the integral. As wished, solving the ODE of D_j first, we now only have to find the integral involving D_j to find the solution of C_j. We proceed with finding the integral involving D_j:

$$\begin{aligned}
\int_0^\tau D_j(s;u)\, ds &\overset{\dagger}{=} \int_0^\tau \frac{b_j - \rho\sigma ui + d_j}{\sigma^2}\frac{1-\exp\{d_j\tau\}}{1-g_j\exp\{d_j\tau\}}\, ds \\
&= \frac{b_j - \rho\sigma ui + d_j}{\sigma^2}\cdot\int_0^\tau \frac{1-\exp\{d_j\tau\}}{1-g_j\exp\{d_j\tau\}}\, ds \\
&\overset{\dagger\dagger}{=} \frac{b_j - \rho\sigma ui + dj}{\sigma^2}\frac{1}{d_j}\cdot\int_1^{\exp\{d_j\tau\}} \frac{1-y}{1-g_jy}\frac{1}{y}\, dy \\
&= \frac{b_j - \rho\sigma ui + dj}{\sigma^2}\frac{1}{d_j}\cdot\int_1^{\exp\{d_j\tau\}} \frac{1-y}{y\,(1-g_jy)}\, dy \\
&= \frac{b_j - \rho\sigma ui + dj}{\sigma^2}\frac{1}{d_j}\cdot\int_1^{\exp\{d_j\tau\}} \frac{1-g_jy-(y-g_jy)}{y\,(1-g_jy)}\, dy \\
&= \frac{b_j - \rho\sigma ui + dj}{\sigma^2}\frac{1}{d_j}\cdot\int_1^{\exp\{d_j\tau\}} \frac{1}{y} - \frac{1-g_j}{1-g_jy}\, dy \\
&= \frac{b_j - \rho\sigma ui + dj}{\sigma^2}\frac{1}{d_j}\cdot\left(\int_1^{\exp\{d_j\tau\}} \frac{1}{y}dy - \int_1^{\exp\{d_j\tau\}} \frac{1-g_j}{1-g_jy}dy\right) \\
&\overset{\dagger\dagger\dagger}{=} \frac{b_j - \rho\sigma ui + dj}{\sigma^2}\frac{1}{d_j}\cdot\left(\left[\log(y)\right]_1^{\exp\{d_j\tau\}} + \frac{1-g_j}{g_j}\left[\log(1-g_jy)\right]_1^{\exp\{d_j\tau\}}\right) \\
&= \frac{b_j - \rho\sigma ui + dj}{\sigma^2}\frac{1}{d_j} \\
&\quad\cdot\left(\left[\log(\exp\{d_j\tau\}) - \log(1)\right] + \frac{1-g_j}{g_j}\left[\log(1-g_j\exp\{d_j\tau\}) - \log(1-g_j)\right]\right) \\
&= \frac{b_j - \rho\sigma ui + dj}{\sigma^2}\frac{1}{d_j}\cdot\left(d_j\tau + \frac{1-g_j}{g_j}\log\left(\frac{1-g_j\exp\{d_j\tau\}}{1-g_j}\right)\right),
\end{aligned}$$

where † follows from our just found expression for D_j, †† from substition using:

$$y = \exp\{d_j s\}, \quad dy = d_j\exp\{d_j s\}\, ds, \quad ds = \frac{dy}{d_j y},$$

and the fact that when at $\tau \Rightarrow \exp\{d_j\tau\} = \exp\{d_j\tau\}$ and at zero $\Rightarrow \exp\{d_j \cdot 0\} = 1$. Lastly, $\dagger\dagger\dagger$ follows from:

$$\begin{aligned}\frac{d}{dy}\frac{1-g_j}{g_j}\log(1-g_jy) &= \frac{1}{1-g_jy}\frac{1-g_j}{g_j}(-g_j)\\ &= -\frac{1-g_j}{1-g_jy}\\ &\Rightarrow\\ -\int\frac{1-g_j}{1-g_jy}\,dy &= \frac{1-g_j}{g_j}\log(1-g_jy)+K, \quad K\in\mathbb{R}.\end{aligned}$$

where in our case the integral is definite and hence no constant K added. We are not quite done as we still need to substitute the found integral back into the expression for C_j:

$$\begin{aligned}C_j &= rui\tau + a\int_0^\tau D_j(s;u)\,ds.\\ &= rui\tau + a\frac{b_j-\rho\sigma ui+d_j}{\sigma^2}\frac{1}{d_j}\cdot\left(d_j\tau+\frac{1-g_j}{g_j}\log\left(\frac{1-g_j\exp\{d_j\tau\}}{1-g_j}\right)\right)\\ &= rui\tau + \frac{a}{\sigma^2}\cdot\left((b_j-\rho\sigma ui+d_j)\tau+\frac{1}{d_j}(b_j-\rho\sigma ui+d_j)\frac{1-g_j}{g_j}\log\left(\frac{1-g_j\exp\{d_j\tau\}}{1-g_j}\right)\right)\\ &\overset{\dagger}{=} rui\tau + \frac{a}{\sigma^2}\cdot\left((b_j-\rho\sigma ui+d_j)\tau+\frac{1}{d_j}(b_j-\rho\sigma ui+d_j)\frac{1-\frac{\rho\sigma ui-b_j-d_j}{\rho\sigma ui-b_j+d_j}}{\frac{\rho\sigma ui-b_j-d_j}{\rho\sigma ui-b_j+d_j}}\log\left(\frac{1-g_j\exp\{d_j\tau\}}{1-g_j}\right)\right)\\ &= rui\tau + \frac{a}{\sigma^2}\cdot\left((b_j-\rho\sigma ui+d_j)\tau+\frac{1}{d_j}(b_j-\rho\sigma ui+d_j)\frac{(\rho\sigma ui-b_j+d_j)-(\rho\sigma ui-b_j-d_j)}{\rho\sigma ui-b_j-d_j}\log\left(\frac{1-g_j\exp\{d_j\tau\}}{1-g_j}\right)\right)\\ &= rui\tau + \frac{a}{\sigma^2}\cdot\left((b_j-\rho\sigma ui+d_j)\tau+\frac{1}{d_j}(b_j-\rho\sigma ui+d_j)\frac{2d_j}{\rho\sigma ui-b_j-d_j}\log\left(\frac{1-g_j\exp\{d_j\tau\}}{1-g_j}\right)\right)\\ &= rui\tau + \frac{a}{\sigma^2}\cdot\left((b_j-\rho\sigma ui+d_j)\tau-\frac{1}{d_j}2d_j\frac{\rho\sigma ui-b_j-d_j}{\rho\sigma ui-b_j-d_j}\log\left(\frac{1-g_j\exp\{d_j\tau\}}{1-g_j}\right)\right)\\ &= rui\tau + \frac{a}{\sigma^2}\cdot\left((b_j-\rho\sigma ui+d_j)\tau-2\log\left(\frac{1-g_j\exp\{d_j\tau\}}{1-g_j}\right)\right),\end{aligned}$$

where $\dagger$ follows from $g_j := x_{j,-}/x_{j,+}$.

1.3 Numerical implementation of characteristic functions

⋆ All the code can be viewed in Appendix A.

⋆ From Havrylenko (2024), pp. 59-65 we define a function to compute the characteristic functions Ψ_j, $j = 1, 2$, given by:

$$\Psi^j_{x(T)}(x, v, \tau; u) = \exp\left\{C_j(\tau; u) + D_j(\tau; u) \cdot v + iux\right\},$$

with:

$$\begin{aligned}
C(\tau; u) &= rui\tau + \frac{a}{\sigma^2}\left((b_j - \rho\sigma ui + d_j)\tau - 2\log\left(\frac{1 - g_j e^{d_j\tau}}{1 - g_j}\right)\right),\\
D_j(\tau; u) &= \frac{b_j - \rho\sigma ui + d_j}{\sigma^2}\frac{1 - e^{d_j\tau}}{1 - g_j e^{d_j\tau}},\\
g_j &= \frac{b_j - \rho\sigma ui + d_j}{b_j - \rho\sigma ui - d_j},\\
d_j &= \sqrt{(\rho\sigma ui - b_j)^2 - \sigma^2(2u_j ui - u^2)},\\
u_1 &= \frac{1}{2}, \quad u_2 = -\frac{1}{2}, \quad a = \kappa\theta, \quad b_1 = \kappa + \lambda - \rho\sigma, \quad b_2 = \kappa + \lambda,
\end{aligned}$$

that takes parameters seen in Table 1 with given specific values. We define the function in `Python` as `characteristicFunctionHeston`. All the requirements are met with the function parameter `j` to choose which characteristic function to compute (and draw corresponding C_j, D_j, g_j, d_j and u, b formulas from the chosen `j`).

Description	**Symbol**	**Value**
Current Stock Price	S_t	100
Current Variance	v_t	0.06
Risk-free Interest Rate	r	0.05
Speed of Mean Reversion	κ	1
Long-term Mean of Variance	θ	0.06
Volatility of the Volatility	σ	0.3
Correlation Coefficient	ρ	-0.5
Market Price of Risk	λ	0.01
Time to Expiry	τ	1

Table 1: Parameters for computing the characteristic functions Ψ_1, Ψ_2.

The plot seen in Figure 1 is of the real and imaginary part of Ψ_j, $j = 1, 2$ computed using the above defined function in `Python`. The pattern for the real and imaginary part is seen, as oscillating with peaks (maximum amplitudes) around the middle of the interval for $u \in [-20, 20]$, i.e near $u \approx 0$, and lower amplitude oscillations around the ends, i.e near $u \approx \pm 20$. More specifically, we see that the real part of the characteristic functions is even but the imaginary part is odd. The graph of $\mathfrak{Im}(\Psi_j)$ has odd symmetry, meaning it has a rotational symmetry about the origin, and the graph of $\mathfrak{Re}(\Psi_j)$ has even symmetry, meaning it has symmetry about the second axis - although it requires some *imagination* to see said symmetry as the second axis is not centered.

Real and Imaginary Parts of $\Psi_1(u)$ and $\Psi_2(u)$ for $u \in [-20, 20]$

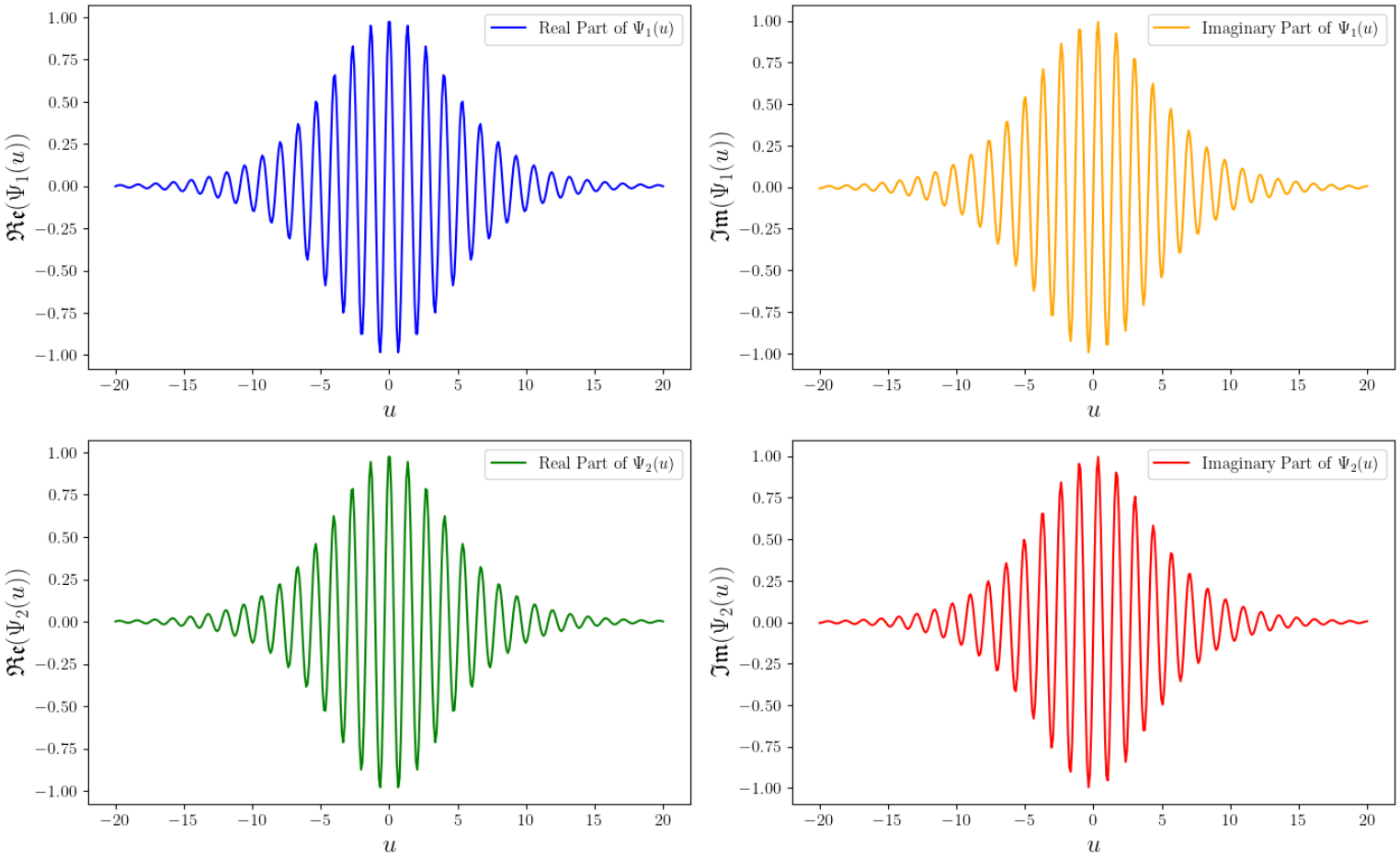

Figure 1: Real and imaginary part of Ψ_j, $j = 1, 2$ for $u \in [-20, 20]$.

2 Option pricing in the context of the Heston model

We will report results with five significant figures throughout this section of the HandIn. Computation times will be recorded in *seconds (s)*. When references are given to (x.y) (for example 2.1) it is to be understood as Subsection (x.y) (subsection 2.1) unless otherwise stated.

2.1 Monte Carlo and Euler discretization Scheme

⋆ All the code can be viewed in Appendix A.

⋆ We simulate S_t and v_t under $\tilde{\mathbb{Q}}$ over the time interval $[0, T]$ (to and including expiry), which we assume to be discretized as $0 = t_1 < t_2 < \ldots < t_m = T$, where the time increments are equally spaced with width dt. For $n \in \mathbb{N}$ we use the Euler discretization on an equidistan time grid $\left\{t_i = \frac{iT}{n} \mid i = 0, \ldots, n\right\}$, where n is the number of time points after $t = 0$. From Rouah (2024), p. 4 we start with the initial values S_0 for the stock price and v_0 for the variance. Given a value for v_t at time t (remember $t_1 = 0$), we first obtain the discretization of v_t by v_{t+dt} from:

$$v_{t+dt} = v_t + \kappa(\theta - v_t)dt + \sigma\sqrt{v_t dt}Z_v^{\mathbb{P}},$$

and we obtain the discretization of S_t by S_{t+dt} from:

$$S_{t+dt} = S_t + rS_t dt + \sqrt{v_t dt}S_t Z_s^{\mathbb{P}},$$

where to generate $Z_v^{\mathbb{P}}$ and $Z_s^{\mathbb{P}}$ with correlation ρ, we first generate two independent standard normal variables $Z_1^{\mathbb{P}}$ and $Z_2^{\mathbb{P}}$, and set $Z_v^{\mathbb{P}} = Z_1^{\mathbb{P}}$ and $Z_s^{\mathbb{P}} = \rho Z_1^{\mathbb{P}} + \sqrt{1-\rho^2}Z_2^{\mathbb{P}}$ by Cholesky decomposition Havrylenko (2024), p. 43.

For an arbitrary but fixed λ (i.e no estimation of λ needed) we follow as suggested by Heston (1993) (see Havrylenko (2024), p. 45) the adjusments that preserve the structure v in the Heston model as we want to preform a change of measure from $\mathbb{P}$ to $\tilde{\mathbb{Q}}$ corresponding to λ:

$$\tilde{\kappa} = \kappa + \lambda \quad \text{and} \quad \tilde{\theta} = \frac{\kappa\theta}{\kappa + \lambda},$$

and thus:

$$\begin{aligned} S_{t+dt} &= S_t + rS_t dt + \sqrt{v_t dt}S_t Z_s^{\tilde{\mathbb{Q}}}, \\ v_{t+dt} &= v_t + \tilde{\kappa}(\tilde{\theta} - v_t)dt + \sigma\sqrt{v_t dt}Z_v^{\tilde{\mathbb{Q}}}, \end{aligned}$$

yielding that we simulate under the equivalent Martingale measure $\tilde{\mathbb{Q}}(\lambda)$ for that one path, i.e choosing a different arbitrary $\lambda^\star \neq \lambda$ would yield another equivalent Martingale measure $\tilde{\mathbb{Q}}(\lambda^\star)$ corresponding to $\lambda^\star$. This leads to analytically tractable results for option pricing.

Lastly, we note that there might occure negative v-values at some of the time points due to discretization errors **even** if the Feller condition is met (see Havrylenko (2024), p. 28). When this occurs we use a full truncation scheme, namely, $\max\{0, v_t\}$ but firstly count it towards our 0-Variance-Count for later reporting. In the code we actually simply check using a `if`-statement if the variance at time t_i is less than or equal to 0 - if not - its counted and then forced to 0. The function `generateHestonPathEulerDisc` implements the beforementioned theory as wished in the HandIn #3 description.

The simulation in `Python` is done with the parameters seen in Table 2.

Parameter	**Symbol**	**Value**
Initial Stock Price	S_0	100
Initial Variance	v_0	0.06
Risk-free Interest Rate	r	0.05
Speed of Mean Reversion	κ	1
Long-term Mean of Variance	θ	0.06
Volatility of the Volatility	σ	0.3
Correlation Coefficient	ρ	-0.5
Market Price of Risk	λ	0.01
Expiry Time	T	1
Strike Price	K	100
Number of Time Points	n	100
Number of Paths	N	1000

Table 2: Simulation and model parameters for the Heston model to calculate the European call option price using the Monte Carlo and Euler discretization scheme.

The results from simulation using the pricing-function `priceHestonCallViaEulerMC` for three different seeds (`np.random.seed()`) is seen in Table 3. We use the `generateHestonPathEulerDisc`-function to simulate N paths and then estimate prices of the European call option on the underlying asset S following a Heston model by discounting the mean of the payoffs of the N paths as this would yield prices near the expectation under $\tilde{\mathbb{Q}}$ corresponding to λ by the Law of Large Numbers (LLN) - as we do in Monte Carlo estimates.

Euler Monte Carlo			
	Seed A	**Seed B**	**Seed C**
Option Price	12.247	11.849	11.781
Standard Deviation	0.51792	0.51211	0.52947
Computing Time	0.70570	0.61735	0.70212
0-Variance-Count	52	47	36

Table 3: Simulation results using Euler Monte Carlo discretization for seeds $\mathbf{A} = 1$, $\mathbf{B} = 10$ and $\mathbf{C} = 100$.

Observe that the option price depends upon the seed-number which implies that the Monte Carlo, and specifically Euler discretization, scheme might not be precise enough for actual option pricing. Furthermore, we kept the number of simulations fixed, as requested. If this constraint was lifted and simulation was done at a higher number of paths the results for every seed would differ as well. These findings for Monte Carlo follow exactly as given by Havrylenko (2024), p. 73.

2.2 Monte Carlo and Milstein discretization scheme

⋆ All the code can be viewed in Appendix A.

⋆ We refer to the logical build up for the functions used in 2.1 but shortly explain the implementation of Monte Carlo method but now with the Milstein discretization scheme. Initial values S_0 and v_0 are given. From Rouah (2024), p. 8, given a value for v_t at time t, we first obtain the discretization of v_t by v_{t+dt} from:

$$v_{t+dt} = v_t + \kappa(\theta - v_t)dt + \sigma\sqrt{v_t dt}Z_v^{\mathbb{P}} + \frac{1}{4}\sigma^2 dt\left((Z_v{}^{\mathbb{P}})^2 - 1\right),$$

and we obtain the discretization of S_t by S_{t+dt} from:

$$S_{t+dt} = S_t + rS_t dt + \sqrt{v_t dt}S_t Z_s^{\mathbb{P}} + \frac{1}{4}S_t^2 dt\left((Z_s{}^{\mathbb{P}})^2 - 1\right),$$

where to generate $Z_v^{\mathbb{P}}$ and $Z_s^{\mathbb{P}}$ with correlation ρ, we first generate two independent standard normal variables $Z_1^{\mathbb{P}}$ and $Z_2^{\mathbb{P}}$, and set $Z_v^{\mathbb{P}} = Z_1^{\mathbb{P}}$ and $Z_s^{\mathbb{P}} = \rho Z_1^{\mathbb{P}} + \sqrt{1-\rho^2}Z_2^{\mathbb{P}}$ by Cholesky decomposition Havrylenko (2024), p. 43.

For an arbitrary but fixed λ (i.e no estimation of λ needed) we follow as suggested by Heston (1993) (see Havrylenko (2024), p. 45) the adjusments that preserve the structure v in the Heston model as we want to preform a change of measure $\mathbb{P}$ to $\tilde{\mathbb{Q}}$ corresponding to λ (as explained in EulerMC (2.1)):

$$\tilde{\kappa} = \kappa + \lambda \quad \text{and} \quad \tilde{\theta} = \frac{\kappa\theta}{\kappa + \lambda},$$

and thus:

$$\begin{aligned} S_{t+dt} &= S_t + rS_t dt + \sqrt{v_t dt}S_t Z_s^{\tilde{\mathbb{Q}}} + \frac{1}{4}S_t^2 dt\left((Z_s^{\tilde{\mathbb{Q}}})^2 - 1\right) \\ v_{t+dt} &= v_t + \tilde{\kappa}(\tilde{\theta} - v_t)dt + \sigma\sqrt{v_t dt}Z_v^{\tilde{\mathbb{Q}}} + \frac{1}{4}\sigma^2 dt\left((Z_v^{\tilde{\mathbb{Q}}})^2 - 1\right). \end{aligned}$$

The simulation in `Python` is done with the parameters seen in Table 4.

Parameter	Symbol	Value
Initial Stock Price	S_0	100
Initial Variance	v_0	0.06
Risk-free Interest Rate	r	0.05
Speed of Mean Reversion	κ	1
Long-term Mean Variance	θ	0.06
Volatility of the Volatility	σ	0.3
Correlation Coefficient	ρ	-0.5
Market Price of Risk	λ	0.01
Expiry Time	T	1
Strike Price	K	100
Number of Time Points	n	100
Number of Paths	N	1000

Table 4: Simulation and model parameters for the Heston model to calculate the European call option price using the Monte Carlo and Milstein discretization scheme.

The results from simulation in `Python` for three different seeds (`np.random.seed()`) is seen in Table 5. The logical build up of `generateHestonPathMilsteinDisc` and `priceHestonCallViaMilsteinMC` is **exactly** thoes given in EulerMC (2.1) but with the different discretization scheme. We therefore spare you the explanation once more.

Milstein Monte Carlo			
	Seed A	**Seed B**	**Seed C**
Option Price	12.253	11.827	11.778
Standard Deviation	0.51785	0.51029	0.52915
Computing Time	0.75349	0.78604	0.92265
0-Variance-Count	0	0	0

Table 5: Simulation results using Monte Carlo and Milstein discretization for seeds $\mathbf{A} = 1$, $\mathbf{B} = 10$ and $\mathbf{C} = 100$.

The option prices, standard deviations and computing time are of the same ball park as the ones given in 2.1 (EulerMC) and thus subject to the same criticism in terms of seed- and path-dependency. It should be noted that computation time is highly reliant on the state of your computer at that given moment and the drag on your CPU/GPU from other applications

However, of much importance, note that the 0-Variance-Count is 0 for all three seeds. This means that the Milstein discretization scheme seems to produce roughly the same issues as the Euler discretization with the important difference of producing far fewer (here, none) instances of a variance having to be truncated to 0. These findings for Monte Carlo follow as given by Havrylenko (2024), p. 73 and the observation for the 0-Variance-Count is exactly as mentioned by Rouah (2024), p. 7.

The reason for the difference in 0-Variance-Count is that the key to the Milstein Scheme is that the accuracy of the discretization is increased by considering expansion of both $\mu_t = \mu(S_t)$ and $\sigma_t = \sigma(S_t)$ and - specifically - $\mu_t = \mu(v_t)$ and $\sigma_t = \sigma(v_t)$ by Ito's lemma. This expansion of

$\mu_t = \mu(v_t)$ and $\sigma_t = \sigma(v_t)$ adds a correction-term which differs from EulerMC (2.1):

$$v_{t+dt} = \underbrace{v_t + \tilde{\kappa}(\tilde{\theta} - v_t)dt + \sigma\sqrt{v_t dt}Z_v^{\tilde{\mathbb{Q}}}}_{\text{EulerMC discretization scheme}} + \underbrace{\frac{1}{4}\sigma^2 dt\left((Z_v^{\tilde{\mathbb{Q}}})^2 - 1\right)}_{\text{correction}},$$

$$S_{t+dt} = \underbrace{S_t + rS_t dt + \sqrt{v_t dt}S_t Z_s^{\tilde{\mathbb{Q}}}}_{\text{EulerMC discretization scheme}} + \underbrace{\frac{1}{4}S_t^2 dt\left((Z_s^{\tilde{\mathbb{Q}}})^2 - 1\right)}_{\text{correction}}.$$

However, even though no instances required truncation of the variance to 0 under these three seeds, the full truncation scheme must still be applied to v_{t+dt} as this is not a guarantee even though one might be tempted to draw such conclusion based on the above simulation results. Some seeds may (and do) produce 0-Variance-Count under the MilsteinMC discretization scheme.

2.3 Heston's original formula

⋆ All the code can be viewed in Appendix A.

⋆ In this subsection we employ Heston's original formula to compute the price of the European call option on the underlying asset S following the Heston model. From Havrylenko (2024), pp. 59-66, analogous to Subsection (1.3), we define a function `characteristicFunctionHeston` to compute the characteristic functions Ψ_j, $j = 1, 2$, given by:

$$\Psi^j_{x(T)}(x, v, \tau; u) = \exp\left\{C_j(\tau; u) + D_j(\tau; u) \cdot v + iux\right\},$$

with:

$$\begin{aligned}
C_j(\tau; u) &= rui\tau + \frac{a}{\sigma^2}\left((b_j - \rho\sigma ui + d_j)\tau - 2\log\left(\frac{1 - g_j e^{d_j\tau}}{1 - g_j}\right)\right),\\
D_j(\tau; u) &= \frac{b_j - \rho\sigma ui + d_j}{\sigma^2}\frac{1 - e^{d_j\tau}}{1 - g_j e^{d_j\tau}},\\
g_j &= \frac{b_j - \rho\sigma ui + d_j}{b_j - \rho\sigma ui - d_j},\\
d_j &= \sqrt{(\rho\sigma ui - b_j)^2 - \sigma^2(2u_j ui - u^2)},\\
u_1 &= \frac{1}{2}, \quad u_2 = -\frac{1}{2}, \quad a = \kappa\theta, \quad b_1 = \kappa + \lambda - \rho\sigma, \quad b_2 = \kappa + \lambda.
\end{aligned}$$

Using the characteristic function, the price of the European call option under $\tilde{\mathbb{Q}}$ in the Heston model corresponding to λ using Heston's original formula is given by Havrylenko (2024), p. 66 as:

$$Call^{\text{OriginalFT}}(t) = S_t Q_1(\log(S(t)), v(t), t; \log(K)) - Ke^{-r\tau}Q_2(\log(S(t)), v(t), t; \log(K)),$$

where for $j = 1, 2$:

$$Q_j(\log(S(t)), v(t), t; \log(K)) = \frac{1}{2} + \frac{1}{\pi}\int_0^{+\infty} \mathfrak{Re}\left(\frac{e^{-iu\log(K)}\Psi^j_{\log(S(T))}(\log(S(t)), v(t), t; u)}{iu}\right) du.$$

In theory we do not need to consider the real part of the integral but as we need (:in our implementation) to truncate the integral the need arises as there will be an imaginary part.

Pricing of the call option is calculated using the parameters seen in Table 6.

Parameter	**Symbol**	**Value**
Initial Stock Price	S_0	100
Initial Variance	v_0	0.06
Risk-free Interest Rate	r	0.05
Speed of Mean Reversion	κ	1
Long-term Mean of Variance	θ	0.06
Volatility of the Volatility	σ	0.3
Correlation Coefficient	ρ	-0.5
Market Price of Risk	λ	0.01
Time to Expiry	τ	1
Strike Price	K	100

Table 6: Model parameters for the Heston model to calculate the European call option price using Heston's original formula.

However, as noted in Havrylenko (2024), p. 66, computation of the above integrals in Q_j, $j = 1, 2$, can be numerically tricky because of log in C_j as the log has a branch cut along the negative real axis that most numerical integration software packages has difficulty with unlike the root function in d_j (see for example Albrecher et al. (2006) for their description of the axis of evil). To overcome this obstacle and evaluate the integral numerically we employ the `quad`-function. The `quad`-function in `Python`'s `scipy.integrate`-module Virtanen et al. (2020) performs numerical integration of Q_j, $j = 1, 2$ over a specified (truncated) interval using adaptive quadrature methods from the `QUADPACK`-library. We evaluate both integrals in increase upper bounds and then compare the European call price and computation time with the results obtained from 2.1 (EulerMC) and 2.2 (MilsteinMC).

The results can be seen in Table 7 with different increasing upper bounds, u_{max}.

Heston's Original Formula				
	Bounds $[0, 10]$	**Bounds** $[0, 50]$	**Bounds** $[0, 100]$	**Bounds** $[0, 1000]$
Option Price	11.8122	11.936	11.936	11.936
Computing Time	1.0023×10^{-3}	2.9919×10^{-3}	4.9834×10^{-3}	7.9796×10^{-3}

Table 7: Heston's original formula results using numerical integration with different (truncated) upper bounds: $[0, 10]$, $[0, 50]$, $[0, 100]$ and $[0, 1000]$.

Table 7 results show that the option prices computed by Heston's original formula through numerical integration are rougly the same as the ones from EulerMC (2.1) and MilsteinMC (2.2). An important notice is with the increasing upper bound we seem to (at seven significant figures) achieve the same option price. Furthermore this option price is not reliant on a seed. Aiming for a unique price for the European call option, the features of not depending on a seed and achieving a quickly stabilizing price as the upper bound increases are advantageous. Both of these two properties were lacking in EulerMC (2.1) and MilsteinMC (2.2), however, do note that the call price is in the same ball park which does mean they could be used for exotic option pricing.

The major difference in Heston's original formula compared to EulerMC (2.1) and MilsteinMC (2.2) lies in the computating time. We see differences of up to - and exceeding - a factor of 100 be-

tween the computing times of Heston's original formula relative to EulerMC (2.1) and MilsteinMC (2.2). Note however the computation time is indeed, and as expected, increasing in the bounds of integration but so would the increase in paths for EulerMC (2.1) and MilsteinMC (2.2). Advantagously, observe how precise Heston's original formula is for a relatively small upper bounds and increasing the upper bound further seems to not effect the option price up to five significant figures.

It should again be noted that computation time is highly reliant on the state of your computer at that given moment and the drag on your CPU/GPU.

2.4 Carr-Madan formula

⋆ All the code can be viewed in Appendix A.

⋆ In this subsection we employ Carr-Madan approach to Fourier transform pricing to compute the price of the European call option on the underlying asset S following the Heston model. From Havrylenko (2024), 59-66, analogous to Subsections (1.3) and (2.3), we have the characteristic functions Ψ_j, $j = 1, 2$, given by:

$$\Psi^j_{x(T)}(x, v, \tau; u) = \exp\left\{C_j(\tau; u) + D_j(\tau; u) \cdot v + iux\right\},$$

with:

$$\begin{aligned}
C_j(\tau; u) &= rui\tau + \frac{a}{\sigma^2}\left((b_j - \rho\sigma ui + d_j)\tau - 2\log\left(\frac{1 - g_j e^{d_j\tau}}{1 - g_j}\right)\right),\\
D_j(\tau; u) &= \frac{b_j - \rho\sigma ui + d_j}{\sigma^2}\frac{1 - e^{d_j\tau}}{1 - g_j e^{d_j\tau}},\\
g_j &= \frac{b_j - \rho\sigma ui + d_j}{b_j - \rho\sigma ui - d_j},\\
d_j &= \sqrt{(\rho\sigma ui - b_j)^2 - \sigma^2(2u_j ui - u^2)},\\
u_1 &= \frac{1}{2}, \quad u_2 = -\frac{1}{2}, \quad a = \kappa\theta, \quad b_1 = \kappa + \lambda - \rho\sigma, \quad b_2 = \kappa + \lambda.
\end{aligned}$$

However, using the characteristic function the price of the European call option under $\tilde{\mathbb{Q}}$ in the Heston model corresponding to λ using Carr-Madan's Fourier transform formula is given on Havrylenko (2024), p. 77 by (denoting $k := \log K$):

$$Call^{\text{CarrMadan}}(k) = \frac{e^{-\alpha k}}{\pi}\mathfrak{Re}\left(\int_0^{+\infty}\frac{e^{-iuk}e^{-rT}\Psi_{x(T)}\left(u - (1+\alpha)i\right)}{\alpha^2 + \alpha - u^2 + i(1+2\alpha)u}\,du\right).$$

In other words, only one integration scheme is required in opposition to two in Heston's original formula (2.3) and we thus need to ensure we correctly transition from $\mathbb{P}$ to $\tilde{\mathbb{Q}}$ using the correct Ψ_j, $j = 1, 2$. So, from Havrylenko (2024), pp. 56-57 we see that Q_2 is related to the measure $\tilde{\mathbb{Q}}$ whereas for Q_1 we change measure to $\mathbb{Q}^S$. i.e to elaborate: we have that the price of a European call option can be written as (by change of numeraire):

$$\begin{aligned}
Call(t) &= e^{-r\tau}\mathbb{E}\left((S_T - K)^+\right)\\
&= e^{-r\tau}\mathbb{E}\left((S_T - K)1_{S_T \geq K}\right)\\
&= e^{-r\tau}\mathbb{E}^{\tilde{\mathbb{Q}}}\left(S_T 1_{S_T \geq K}\right) - Ke^{-r\tau}\mathbb{E}^{\tilde{\mathbb{Q}}}\left(1_{S_T \geq K}\right)\\
&= S_t\mathbb{E}^{\tilde{\mathbb{Q}}}\left(\frac{S_T/S_t}{B_T/B_t}1_{S_T \geq K}\right) - Ke^{-r\tau}\mathbb{E}^{\tilde{\mathbb{Q}}}\left(1_{S_T \geq K}\right)\\
&= S_t\mathbb{E}^{\mathbb{Q}^S}\left(\frac{d\tilde{\mathbb{Q}}}{d\mathbb{Q}^S}\frac{S_T/S_t}{B_T/B_t}1_{S_T \geq K}\right) - Ke^{-r\tau}\mathbb{E}^{\tilde{\mathbb{Q}}}\left(1_{S_T \geq K}\right)\\
&= S_t\mathbb{E}^{\mathbb{Q}^S}\left(1_{S_T \geq K}\right) - Ke^{-r\tau}\mathbb{E}^{\tilde{\mathbb{Q}}}\left(1_{S_T \geq K}\right)\\
&= S_t\mathbb{Q}^S(S_T \geq K) - Ke^{-r\tau}\tilde{\mathbb{Q}}(S_T \geq K)\\
&= S_t\mathbb{Q}^S(\log S_T \geq \log K) - Ke^{-r\tau}\tilde{\mathbb{Q}}(\log S_T \geq \log K)\\
&= S_t Q_1 - Ke^{-r\tau}Q_2,
\end{aligned}$$

where $\frac{d\tilde{\mathbb{Q}}}{d\mathbb{Q}^S}$ is the Radon-Nikodym derivative given by $\frac{d\tilde{\mathbb{Q}}}{d\mathbb{Q}^S} = (B_T/B_t)/(S_T/S_t)$ as $\tilde{\mathbb{Q}}$ uses the bond B_t as the numeraire, while the measure $\mathbb{Q}^S$ uses the stock price S. Resultingly, Q_2 is the correct function as it relates to $\tilde{\mathbb{Q}}$ and thus Ψ_2 the correct characteristic function to use in the Carr-Madan European call option formula. Ψ_1 can be used but has to be implemented differently (see Havrylenko (2024), p. 71). Consequently, when implementing the `characteristicFunctionHeston` into the evaluation of the integral in the Carr-Madan Fourier transform pricing formula for the European call option, we restrict `j=2` in the function parameter. Furthermore, the horizontal shift for the characteristic function argument is also restricted to `(u-(1+alpha)i)` as opposed to `u` (see above formula for Carr-Madan).

In theory we do not need to consider the real part of the integral but as we need (:in our implementation) to truncate the integral for numerical evaluation the need arises as there will be an imaginary part.

To evaluate the integral numerically we employ the `quad`-function in `Python`, again (see subsection 2.4 for the same description of the axis of evil from the log-function).

Pricing of the call option is then calculated using the parameters seen in Table 8.

Parameter	**Symbol**	**Value**
Initial Stock Price	S_0	100
Initial Variance	v_0	0.06
Risk-free Interest Rate	r	0.05
Speed of Mean Reversion	κ	1
Long-term Mean of Variance	θ	0.06
Volatility of the Volatility	σ	0.3
Correlation Coefficient	ρ	-0.5
Market Price of Risk	λ	0.01
Time to Expiry	τ	1
Strike Price	K	100
Damping Factor	α	0.3

Table 8: Model parameters for the Heston's model European call option pricing using Carr-Madan's Fourier transfom approach.

The results can be seen in Table 9 with different increasing upper bounds and specifically $u_{max} = 50$ as requested in the HandIn #3.

Carr-Madan's Fourier Transform Formula				
	Bounds $[0, 10]$	**Bounds** $[0, 50]$	**Bounds** $[0, 100]$	**Bounds** $[0, 1000]$
Option Price	11.886	11.936	11.936	11.936
Computing Time	3.9701×10^{-3}	6.0089×10^{-3}	5.985×10^{-3}	8.9772×10^{-3}

Table 9: Carr-Madan's Fourier transform results using numerical integration with different (truncated) upper bounds: $[0, 10]$, $[0, 50]$, $[0, 100]$ and $[0, 1000]$.

Firstly, observe that the results of (2.4) are almost identical to thoes of (2.3). We will however comment on why this might not be a general result when we increase the number of call option

calculations or if the computation was done under the same CPU/GPU-drag.

If we were to price a large number of options we would expect the Carr-madan method (2.4) to be faster in terms of computing time compared to that of Heston's formula (2.3) and especially thoes of EulerMC (2.1) and MilsteinMC (2.2). To see why consider both call option pricing formulas for (2.3):

$$Call^{\text{OriginalFT}}(t) = S_t Q_1(\log(S(t)), v(t), t; \log(K)) - Ke^{-r\tau} Q_2(\log(S(t)), v(t), t; \log(K)),$$

and for (2.4) denoting $k := \log K$:

$$Call^{\text{CarrMadan}}(k) = \frac{e^{-\alpha k}}{\pi} \mathfrak{Re} \left(\int_0^{+\infty} \frac{e^{-iuk} e^{-rT} \Psi_{x(T)} \left(u - (1+\alpha)i\right)}{\alpha^2 + \alpha - u^2 + i(1+2\alpha)u} \, du \right).$$

Notice that the denominator of the Carr-Madan formula (2.3) decays the integral relatively faster compared to that of Heston's original formula (2.4), because the integrand enters in the denominator squared in Carr-Madan formula (2.3) where as it enters linearly in the denominator in Heston's original formula (2.4). Another obvious advantageous is the fact that we have one integration scheme in Carr-Madan formula (2.3) as opposed to two in Heston's original formula (2.4) which for a larger number of options could be significant.

The key difference between Carr-Madan's formula and the methods EulerMC (2.1) and MilsteinMC (2.2) is the computation time, with Carr-Madan's formula being faster by up to a factor of 100 compared to EulerMC (2.1) and MilsteinMC (2.2). Despite the expected increase in computation time with wider integration bounds Carr-Madan's (2.2) precision remains high for small upper bounds without significantly affecting option prices by up to atleast five decimal points.

It should again be noted as it is not negliable whatsoever that the computation time is highly reliant on the state of your computer at that given moment and the drag on your CPU/GPU.

In summary of question 2 we can easily conclude the following from experimentation (and theory):

- All the methods lead to prices around the same ball park.
- The Fourier transform based methods ((2.3) and (2.4)) were significantly faster at computing option prices of up to and exceeding a factor of 100 compared to EulerMC (2.1) and MilsteinMC (2.2).
- MilsteinMC (2.2) was identical to EulerMC (2.3) with the important difference of almost no occurences of 0-Variance-Count in the former method because of the expansions of $\mu(v_t)$ and $\sigma(v_t)$.
- EulerMC (2.1) and MilsteinMC (2.2) were both not precise enough methods for option pricing based on seed- and path-dependence.
- Carr-Madan (2.4) would be compared to Heston (2.3) as in the former the denominator in the integral contains u^2 as opposed to u in the latter method. This could be significant for heavy computational option calculations that we did not consider here. Anecdotally, Yevhen's dissertation used Carr-Madan as it was the only sufficiently fast method.

3 Asset allocation under the Heston model

3.1 Derivation of the Hamilton-Jacobi-Bellman PDE

⋆ Consider the set of admissible investment strategies given by $\mathcal{A}(t,x,v)$. The wealth of the risk-averse investor then equals x at time t for $t \leq T$. Consequently, the value function, $\mathcal{V}$, can be written for any $t \in [0,T]$ as:

$$\begin{aligned}\mathcal{V}(t,x,u) &= \max_{\pi \in \mathcal{A}(t,x,v)} \mathbb{E}\left[U(X^\pi(T))\right] \\ &= \max_{\pi \in \mathcal{A}(t,x,v)} \mathbb{E}\left[U(X^\pi(T)) \mid X^\pi(t) = x, v(t) = v\right].\end{aligned}$$

Maximizing expected utility over $\pi \in \mathcal{A}(t,x,v)$ simplifies when $t = T$, as the interval $t \in [0,T]$ simplifies to the single point $t = T$. At $t = T$ the expectation vanishes as the investment horizon is reached and the wealth and variance is thus known. This leads directly to the terminal condition:

$$\begin{aligned}\mathcal{V}(T,x,u) &= \max_{\pi \in \mathcal{A}(t,x,v)} \mathbb{E}\left[U(X^\pi(T)) \mid X^\pi(T) = x, v(T) = v\right] \\ &= \max_{\pi \in \mathcal{A}(T,x,v)} \mathbb{E}\left[U(x)\right] \\ &= U(x).\end{aligned}$$

⋆ We have that the dynamics for the wealth process $X^\pi(t+h)$ and variance $v(t+h)$ for some arbitrary constant investment strategy, π, is given by:

$$\begin{aligned}dX^\pi(t+h) &= X^\pi(t+h)\left(r + \pi\bar{\lambda}v(t+h)\right)d(t+h) + X^\pi(t+h)\pi\sqrt{v(t+h)}dW_1^{\mathbb{P}}(t+h), \\ dv(t+h) &= \kappa\left(\theta - v(t+h)\right)d(t+h) + \sigma\rho\sqrt{v(t+h)}dW_1^{\mathbb{P}}(t+h) + \sigma\sqrt{v(t+h)}\sqrt{1-\rho^2}dW_2^{\mathbb{P}}(t+h).\end{aligned}$$

We now assume - as we are told that $\mathcal{V}$ is sufficiently smooth - that $\mathcal{V}(t,x,u) \in C^{1,2}$ for the purpose of applying multi-dimensional Ito Theorem 4.19 Björk (2020). This yields the dynamics of the value process, $\mathcal{V}(t,x,u)$, for some arbitrary constant investment strategy, π:

$$\begin{aligned}
d\mathcal{V}(t+h, X^\pi(t+h), v(t+h)) &= \mathcal{V}_t d(t+h) + \mathcal{V}_x dX^\pi(t+h) + \mathcal{V}_v dv(t+h) \\
&\quad + \frac{1}{2}\mathcal{V}_{xx}\left(dX^\pi(t+h)\right)^2 + \frac{1}{2}\mathcal{V}_{vv}\left(dv(t+h)\right)^2 \\
&\quad + \frac{1}{2}2\mathcal{V}_{xv}\left(dX^\pi(t+h)\right)\left(dv(t+h)\right) \\
&= \mathcal{V}_t d(t+h) + \mathcal{V}_x X^\pi(t+h)\left(r + \pi\bar{\lambda}v(t+h)\right)d(t+h) \\
&\quad + \mathcal{V}_x X^\pi(t+h)\pi\sqrt{v(t+h)}dW_1^{\mathbb{P}}(t+h) + \mathcal{V}_v\kappa\left(\theta - v(t+h)\right)d(t+h) \\
&\quad + \mathcal{V}_v\sigma\rho\sqrt{v(t+h)}dW_1^{\mathbb{P}}(t+h) + \mathcal{V}_v\sigma\sqrt{v(t+h)}\sqrt{1-\rho^2}dW_2^{\mathbb{P}}(t+h) \\
&\quad + \frac{1}{2}\mathcal{V}_{xx}(X^\pi(t+h))^2\pi^2 v(t+h)d(t+h) + \frac{1}{2}\mathcal{V}_{vv}\sigma^2\rho^2 v(t+h)d(t+h) \\
&\quad + \frac{1}{2}\mathcal{V}_{vv}\sigma^2 v(t+h)\left(1-\rho^2\right)d(t+h) + \mathcal{V}_{xv}X^\pi(t+h)\pi v(t+h)\sigma\rho d(t+h) \\
&= \Bigg(\mathcal{V}_t + \mathcal{V}_x X^\pi(t+h)\left(r + \pi\bar{\lambda}v(t+h)\right) + \mathcal{V}_v\kappa\left(\theta - v(t+h)\right) \\
&\qquad + \frac{1}{2}\mathcal{V}_{xx}(X^\pi(t+h))^2\pi^2 v(t+h) + \frac{1}{2}\mathcal{V}_{vv}\sigma^2 v(t+h) + \mathcal{V}_{xv}X^\pi(t+h)\pi v(t+h)\sigma\rho\Bigg)d(t+h) \\
&\quad + \left(\mathcal{V}_x X^\pi(t+h)\pi\sqrt{v(t+h)} + \mathcal{V}_v\sigma\rho\sqrt{v(t+h)}\right)dW_1^{\mathbb{P}}(t+h) \\
&\quad + \mathcal{V}_v\sigma\sqrt{v(t+h)}\sqrt{1-\rho^2}dW_2^{\mathbb{P}}(t+h),
\end{aligned}$$

where we used the extended multiplication rules $dW_t^i dW_t^i = 0$, $j \neq i$ Björk (2020), p. 61 and the dynamics of both $v(t+h)$ and $X^\pi(t+h)$ as they were stated in the excercise.

By the dynamics found using multi-dimensional Ito we now have that in integral notation:

$$\begin{aligned}
\mathcal{V}(t+h, X^\pi(t+h), v(t+h)) &= \mathcal{V}(t, X^\pi(t), v(t)) \\
&\quad + \int_t^{t+h}\Bigg(\mathcal{V}_t + \mathcal{V}_x X^\pi(s)\left(r + \pi\bar{\lambda}v(s)\right) + V_v\kappa\left(\theta - v(s)\right) \\
&\qquad + \frac{1}{2}\mathcal{V}_{xx}(X^\pi(s))^2\pi^2 v(s) + \frac{1}{2}\mathcal{V}_{vv}\sigma^2 v(s) + \mathcal{V}_{xv}X^\pi(s)\pi v(s)\sigma\rho\Bigg)ds \\
&\quad + \int_t^{t+h}\left(\mathcal{V}_x X^\pi(s)\pi\sqrt{v(s)} + \mathcal{V}_v\sigma\rho\sqrt{v(s)}\right)dW_1^{\mathbb{P}}(s) \\
&\quad + \int_t^{t+h}\mathcal{V}_v\sigma\sqrt{v(s)}\sqrt{1-\rho^2}dW_2^{\mathbb{P}}(s),
\end{aligned}$$

as desired.

$\star$ Substitution of equation (21) into (20) yields:

$$\begin{aligned}
\mathcal{V}(t,x,v) &\geq \mathbb{E}\left(\mathcal{V}(t+h, X^\pi(t+h), v(t+h)) \mid X^\pi(t)=x, v(t)=v\right) \\
&= \mathbb{E}\Bigg(\mathcal{V}(t, X^\pi(t), v(t)) + \int_t^{t+h} \Big(\mathcal{V}_t + \mathcal{V}_x X^\pi(s)\left(r+\pi\bar{\lambda}v(s)\right) + \mathcal{V}_v\kappa\left(\theta - v(s)\right) \\
&\quad + \frac{1}{2}\mathcal{V}_{xx}(X^\pi(s))^2\pi^2 v(s) + \frac{1}{2}\mathcal{V}_{vv}\sigma^2 v(s) + \mathcal{V}_{xv}X^\pi(s)\pi v(s)\sigma\rho\Big)ds \\
&\quad + \int_t^{t+h}\left(\mathcal{V}_x X^\pi(s)\pi\sqrt{v(s)} + \mathcal{V}_v\sigma\rho\sqrt{v(s)}\right)dW_1^{\mathbb{P}}(s) \\
&\quad + \int_t^{t+h}\mathcal{V}_v\sigma\sqrt{v(s)}\sqrt{1-\rho^2}dW_2^{\mathbb{P}}(s) \mid X^\pi(t)=x, v(t)=v\Bigg) \\
&\overset{\dagger}{=} \mathcal{V}(t,x,v) + \mathbb{E}\Big(\int_t^{t+h}\Big(\mathcal{V}_t + \mathcal{V}_x X^\pi(s)\left(r+\pi v(s)\bar{\lambda}\right) + \mathcal{V}_v\kappa\left(\theta - v(s)\right) \\
&\quad + \frac{1}{2}\mathcal{V}_{xx}(X^\pi(s))^2\pi^2 v(s) + \frac{1}{2}\mathcal{V}_{vv}\sigma^2 v(s) + \mathcal{V}_{xv}X^\pi(s)\pi v(s)\sigma\rho\Big)ds \mid X^\pi(t)=x, v(t)=v\Big) \\
&\iff \\
0 &\geq \mathcal{V}(t,x,v) + \mathbb{E}\Bigg(\int_t^{t+h}\Big(\mathcal{V}_t + \mathcal{V}_x X^\pi(s)\left(r+\pi v(s)\bar{\lambda}\right) + \mathcal{V}_v\kappa\left(\theta - v(s)\right) \\
&\quad + \frac{1}{2}\mathcal{V}_{xx}(X^\pi(s))^2\pi^2 v(s) + \frac{1}{2}\mathcal{V}_{vv}\sigma^2 v(s) + \mathcal{V}_{xv}X^\pi(s)\pi v(s)\sigma\rho\Big)ds \mid X^\pi(t)=x, v(t)=v\Bigg) - \mathcal{V}(t,x,v) \\
&= \mathbb{E}\Bigg(\int_t^{t+h}\Big(\mathcal{V}_t + \mathcal{V}_x X^\pi(s)\left(r+\pi v(s)\bar{\lambda}\right) + \mathcal{V}_v\kappa\left(\theta - v(s)\right) \\
&\quad + \frac{1}{2}\mathcal{V}_{xx}(X^\pi(s))^2\pi^2 v(s) + \frac{1}{2}\mathcal{V}_{vv}\sigma^2 v(s) + \mathcal{V}_{xv}X^\pi(s)\pi v(s)\sigma\rho\Big)ds \mid X^\pi(t)=x, v(t)=v\Bigg),
\end{aligned}$$

where † follows from both that: 1) The Brownian motion process is a Martingale implying it beloning to the class $\pounds^2$ and thus yielding conditional expectation zero by proposition 4.8 Björk (2020) 2) The linearity of the expectation operator.

In equation (20), the left-hand side (LHS) delineates the value function under an optimal investment strategy across the interval $[t,T]$. Conversely, the right-hand side (RHS) delineates the value function when adopting any investment strategy during the interval $[t,t+h)$, followed by a shift to an optimal investment strategy for $[t+h,T]$. Thus, the essence of equation (20) is that opting for an arbitrary investment strategy within the interval $[t,t+h)$, before transitioning to an optimal strategy for $[t+h,T]$, is, on average, not superior to consistently adhering to an optimal investment strategy throughout the entire interval $[t,T]$.

$\star$ As stated we want to divide by h, let $h \downarrow 0$. For readability, define the integrand from the previous "$\star$" as:

$$M(s) := \mathcal{V}_t + \mathcal{V}_x X^\pi(s)\left(r+\pi v(s)\bar{\lambda}\right) + \mathcal{V}_v\kappa\left(\theta - v(s)\right) + \frac{1}{2}\mathcal{V}_{xx}(X^\pi(s))^2\pi^2 v(s) + \frac{1}{2}\mathcal{V}_{vv}\sigma^2 v(s) + \mathcal{V}_{xv}X^\pi(s)\pi v(s)\sigma\rho.$$

In other words, rewrite the previous "$\star$" inequality as:

$$0 \geq \mathbb{E}\left(\int_t^{t+h} M(s)\,ds \mid X^\pi(t)=x, v(t)=v\right).$$

Dividing now by h yields:

$$\begin{aligned}
\frac{0}{h} &= 0 \\
&\geq \frac{\mathbb{E}\left(\int_t^{t+h} M(s)\,ds \mid X^\pi(t)=x, v(t)=v\right)}{h} \\
&\overset{\dagger}{=} \frac{\mathbb{E}\left(\int_0^{t+h} M(s)\,ds - \int_0^t M(s)\,ds \mid X^\pi(t)=x, v(t)=v\right)}{h} \\
&\overset{\dagger\dagger}{=} \mathbb{E}\left(\frac{\int_0^{t+h} M(s)\,ds - \int_0^t M(s)\,ds}{h} \mid X^\pi(t)=x, v(t)=v\right),
\end{aligned}$$

where † follows from the additivity and linearity of the integral (as $M(s)$ is a shorthand) and †† from the linearity of the expectation operator. Letting $h \downarrow 0$ now yields:

$$\begin{aligned}
\lim_{h\downarrow 0} 0 &= 0 \\
&\geq \lim_{h\downarrow 0} \mathbb{E}\left(\frac{\int_0^{t+h} M(s)\,ds - \int_0^t M(s)\,ds}{h} \mid X^\pi(t)=x, v(t)=v\right) \\
&\overset{\dagger}{=} \mathbb{E}\left(\lim_{h\downarrow 0} \frac{\int_0^{t+h} M(s)\,ds - \int_0^t M(s)\,ds}{h} \mid X^\pi(t)=x, v(t)=v\right) \\
&\overset{\dagger\dagger}{=} \mathbb{E}\left(\lim_{h\downarrow 0} \frac{f(t+h)-f(t)}{h} \mid X^\pi(t)=x, v(t)=v\right) \\
&= \mathbb{E}\left(f'(t) \mid X^\pi(t)=x, v(t)=v\right) \\
&= \mathbb{E}\left(M(t) \mid X^\pi(t)=x, v(t)=v\right) \\
&\overset{\dagger\dagger\dagger}{=} \mathcal{V}_t + \frac{1}{2}\sigma^2\mathcal{V}_{vv} + \kappa(\theta - v)\mathcal{V}_v + x\left(r + \pi\bar{\lambda}\right)V_x + \frac{1}{2}\pi^2x^2vV_{xx} + \pi x\sigma v\rho V_{xv},
\end{aligned}$$

where † follows from Lebesgue's Dominated Convergence (LDC) as the function $M(s)$ is bounded and †† (and forward) from the definition of a derivative and the Fundamental Theorem of Calculus (FToC) with $f(t) = \int_0^t M(s)\,ds$, implying $f'(t) = M(t)$. † † † is simply from definition using the conditional expectation and unwinding the shorthand notation defined at the start.

⋆ Let π^* represent the optimal investment strategy. It follows that π^* is uniquely determined as the solution to the following optimization problem:

$$g(\pi) := \sup_\pi \left\{ x\left(r + \pi\bar{\lambda}v\right)V_x + \frac{1}{2}\pi^2x^2vV_{xx} + \pi x\sigma v\rho V_{xv} \right\},$$

which signifies that π^* is the supremum of π^* across all conceivable or permissible investment strategies. Furthermore, since the previously found inequality holds for any constant investment strategy π, it follows from the previously found inequality that:

$$0 \geq \mathcal{V}_t + \frac{1}{2}\sigma^2\mathcal{V}_{vv} + \kappa(\theta - v)\mathcal{V}_v + \sup_\pi \left\{ x\left(r + \pi\bar{\lambda}v\right)V_x + \frac{1}{2}\pi^2x^2vV_{xx} + \pi x\sigma v\rho V_{xv} \right\}.$$

Given that π^* is the optimal investment strategy, defined as the supremum over π, it follows that for this π^*, equation (20) must be satisfied with equality. Recall that in equation (20), the left-hand side (LHS) delineates the value function under an optimal investment strategy across the

interval $[t, T]$. Conversely, the right-hand side (RHS) delineates the value function when adopting any investment strategy during the interval $[t, t+h)$, followed by a shift to an optimal investment strategy for $[t+h, T]$. Thus, the essence of equation (20) is that opting for an arbitrary investment strategy within the interval $[t, t+h)$, before transitioning to an optimal strategy for $[t+h, T]$, is, on average, not superior to consistently adhering to an optimal investment strategy throughout the entire interval $[t, T]$. Currently, we find ourselves in a scenario where an optimal strategy is employed over the intervals $[t, t+h)$ and $[t+h, T]$. This approach is tantamount to adhering to an optimal investment strategy throughout the entire period $[t, T]$. Consequently, it is imperative that equation (20) is satisfied with equality for π^*.

We adhere to the mercy of the court to let us re-use the just found dynamics the the previous question for $\mathcal{V}$ (or the fact that Yevhen said it was allowed at the Q&A). Doing the exact same calculations - other than the exact same deriviation for the dynamics - using the optimal investment strategy π^* now yields:

$$\begin{aligned}
\mathcal{V}(t+h, X^{\pi^*}(t+h), v(t+h)) = \mathcal{V}(t, X^{\pi^*}(t), v(t)) \\
&+ \int_t^{t+h} \left(\mathcal{V}_t + \frac{1}{2}\sigma^2 v(s)\mathcal{V}_{vv} + \kappa\left(\theta - v(s)\right)\mathcal{V}_v \right. \\
&\quad \left. + \sup_\pi \left\{ X^{\pi^*}\left(r + \pi\bar{\lambda}v(s)\right)\mathcal{V}_x + \frac{1}{2}\pi^2 (X^{\pi^*})^2 v(s)\mathcal{V}_{xx} + \pi X^{\pi^*}\sigma v(s)\rho\mathcal{V}_{xv} \right\} \right) ds \\
&+ \int_t^{t+h} \left(\sup_\pi \left\{ \mathcal{V}_x X^\pi(s)\pi\sqrt{v(s)} \right\} + \mathcal{V}_v \sigma\rho\sqrt{v(s)} \right) dW_1^{\mathbb{P}}(s) \\
&+ \int_t^{t+h} \mathcal{V}_v \sigma\sqrt{v(s)}\sqrt{1-\rho^2} dW_2^{\mathbb{P}}(s).
\end{aligned}$$

As π^* is the optimal investment strategy, as argued above, we now have that equation (20) must hold with equality:

$$\begin{aligned}
\mathcal{V}(t,x,v) &= \mathbb{E}\left(\mathcal{V}(t+h, X^{\pi^*}(t+h), v(t+h)) \mid X^{\pi^*}(t)=x, v(t)=v\right) \\
&= \mathbb{E}\Bigg(\mathcal{V}(t, X^{\pi^*}(t), v(t)) + \int_t^{t+h} \Bigg(\mathcal{V}_t + \frac{1}{2}\sigma^2 v(s)\mathcal{V}_{vv} + \kappa\left(\theta - v(s)\right)\mathcal{V}_v \\
&\quad + \sup_\pi \left\{ X^{\pi^*}(s)\left(r + \pi\bar{\lambda}v(s)\right)\mathcal{V}_x + \frac{1}{2}\pi^2 (X^{\pi^*}(s))^2 v\mathcal{V}_{xx} + \pi X^{\pi^*}(s)\sigma v(s)\rho\mathcal{V}_{xv}\right\}\Bigg) ds \\
&\quad + \int_t^{t+h} \left(\sup_\pi \left\{\mathcal{V}_x X^{\pi^*}(s)\pi\sqrt{v(s)}\right\} + \mathcal{V}_v\sigma\rho\sqrt{v(s)}\right) dW_1^{\mathbb{P}}(s) \\
&\quad + \int_t^{t+h} \mathcal{V}_v\sigma\sqrt{v(s)}\sqrt{1-\rho^2}dW_2^{\mathbb{P}}(s) \mid X^{\pi^*}(t)=x, v(t)=v\Bigg) \\
&\overset{\dagger}{=} \mathcal{V}(t,x,v) + \mathbb{E}\Bigg(\int_t^{t+h} \Bigg(\mathcal{V}_t + \frac{1}{2}\sigma^2 v(s)\mathcal{V}_{vv} + \kappa\left(\theta - v(s)\right)\mathcal{V}_v \\
&\quad + \sup_\pi \left\{ X^{\pi^*}(s)\left(r + \pi\bar{\lambda}v(s)\right)\mathcal{V}_x + \frac{1}{2}\pi^2 (X^{\pi^*}(s))^2 v(s)\mathcal{V}_{xx} + \pi X^{\pi^*}(s)\sigma v(s)\rho\mathcal{V}_{xv}\right\}\Bigg) ds \mid X^{\pi^*}(t)=x, v(t)=v\Bigg) \\
&\iff \\
0 &= \mathcal{V}(t,x,v) + \mathbb{E}\Bigg(\int_t^{t+h} \Bigg(\mathcal{V}_t + \frac{1}{2}\sigma^2 v(s)\mathcal{V}_{vv} + \kappa\left(\theta - v(s)\right)\mathcal{V}_v \\
&\quad + \sup_\pi \left\{ X^{\pi^*}(s)\left(r + \pi\bar{\lambda}v(s)\right)\mathcal{V}_x + \frac{1}{2}\pi^2 (X^{\pi^*})^2(s) v(s)\mathcal{V}_{xx} + \pi X^{\pi^*}(s)\sigma v(s)\rho\mathcal{V}_{xv}\right\}\Bigg) ds \mid X^{\pi^*}(t)=x, v(t)=v\Bigg) - \\
&= \mathbb{E}\Bigg(\int_t^{t+h} \Bigg(\mathcal{V}_t + \frac{1}{2}\sigma^2 v(s)\mathcal{V}_{vv} + \kappa\left(\theta - v(s)\right)\mathcal{V}_v \\
&\quad + \sup_\pi \left\{ X^{\pi^*}(s)\left(r + \pi\bar{\lambda}v(s)\right)\mathcal{V}_x + \frac{1}{2}\pi^2 (X^{\pi^*})^2 v(s)\mathcal{V}_{xx} + \pi X^{\pi^*}(s)\sigma v(s)\rho\mathcal{V}_{xv}\right\}\Bigg) ds \mid X^{\pi^*}(t)=x, v(t)=v\Bigg),
\end{aligned}$$

where † follows from both that: 1) The Brownian motion process is a Martingale, beloning to the class $\pounds^2$, and thus yielding conditional expectation zero by proposition 4.8 Björk (2020), 2) The linearity of the expectation operator.

In the same manner as the previous "$\star$", define:

$$J(s) := \mathcal{V}_t + \frac{1}{2}\sigma^2 v(s)\mathcal{V}_{vv} + \kappa\left(\theta - v(s)\right)\mathcal{V}_v + \sup_\pi \left\{ X^{\pi^*}(s)\left(r + \pi\bar{\lambda}v(s)\right)\mathcal{V}_x + \frac{1}{2}\pi^2 (X^{\pi^*}(s))^2 v(s)\mathcal{V}_{xx} + \pi X^{\pi^*}(s)\sigma v(s)\right.$$

In other words:

$$0 = \mathbb{E}\left(\int_t^{t+h} J(s)\, ds \mid X^{\pi^*}(t)=x, v(t)=v\right).$$

Dividing now by h yields:

$$\begin{aligned}
\frac{0}{h} &= 0 \\
&= \frac{\mathbb{E}\left(\int_t^{t+h} J(s)\,ds \mid X^{\pi^*}(t) = x, v(t) = v\right)}{h} \\
&\overset{\dagger}{=} \frac{\mathbb{E}\left(\int_0^{t+h} J(s)\,ds - \int_0^t J(s)\,ds \mid X^{\pi^*}(t) = x, v(t) = v\right)}{h} \\
&\overset{\dagger\dagger}{=} \mathbb{E}\left(\frac{\int_0^{t+h} J(s)\,ds - \int_0^t J(s)\,ds}{h} \mid X^{\pi^*}(t) = x, v(t) = v\right),
\end{aligned}$$

where † follows from the additivity and linearity of the integral and †† from the linearity of the expectation. Letting $h \downarrow 0$ now yields:

$$\begin{aligned}
\lim_{h\downarrow 0} 0 &= 0 \\
&= \lim_{h\downarrow 0} \mathbb{E}\left(\frac{\int_0^{t+h} J(s)\,ds - \int_0^t J(s)\,ds}{h} \mid X^{\pi^*}(t) = x, v(t) = v\right) \\
&\overset{\dagger}{=} \mathbb{E}\left(\lim_{h\downarrow 0} \frac{\int_0^{t+h} J(s)\,ds - \int_0^t J(s)\,ds}{h} \mid X^{\pi^*}(t) = x, v(t) = v\right) \\
&\overset{\dagger\dagger}{=} \mathbb{E}\left(\lim_{h\downarrow 0} \frac{f(t+h) - f(t)}{h} \mid X^{\pi^*}(t) = x, v(t) = v\right) \\
&= \mathbb{E}\left(f'(t) \mid X^{\pi^*}(t) = x, v(t) = v\right) \\
&= \mathbb{E}\left(J(t) \mid X^{\pi^*}(t) = x, v(t) = v\right) \\
&\overset{\dagger\dagger\dagger}{=} \mathcal{V}_t + \frac{1}{2}\sigma^2 v \mathcal{V}_{vv} + \kappa(\theta - v)\mathcal{V}_v + \sup_{\pi}\left\{x\left(r + \pi\bar{\lambda}v\right)\mathcal{V}_x + \frac{1}{2}\pi^2 x^2 v \mathcal{V}_{xx} + \pi x \sigma v \rho \mathcal{V}_{xv}\right\},
\end{aligned}$$

where † follows from Lebesgue's Dominated Convergence (LDC) as the function $J(s)$ is bounded and †† (and forward) from the definition of a derivative and the Fundamental Theorem of Calculus (FToC) with $f(t) = \int_0^t J(s)\,ds$, implying $f'(t) = J(t)$. † † † is simply by definition using the conditional expectation and unwinding the shorthand notation defined at the start. The last equality is exactly the Hamilton-Jacobi-Bellman partial differential equation HJB PDE, equation (22)

3.2 Solution to the Hamilton-Jacobi-Bellman PDE

⋆ The definition of the function $g(\pi)$ is seen in the underbrace of equation (22). We find the FOC of g:

$$\begin{aligned}
g'(\pi) = x\bar{\lambda}v\mathcal{V}_x + \frac{1}{2}2\pi x^2 v\mathcal{V}_{xx} + x\sigma v\rho\mathcal{V}_{xv} &= 0 \\
&\overset{\dagger}{\iff} \\
\bar{\lambda}\mathcal{V}_x + \pi x\mathcal{V}_{xx} + \sigma\rho\mathcal{V}_{xv} &= 0 \\
&\iff \\
-\bar{\lambda}\mathcal{V}_x - \sigma\rho\mathcal{V}_{xv} &= \mathcal{V}_{xx}\pi x \\
&\iff \\
\pi &= -\frac{\bar{\lambda}\mathcal{V}_x}{x\mathcal{V}_{xx}} - \frac{\sigma\rho\mathcal{V}_{xv}}{x\mathcal{V}_{xx}} \\
&\overset{\dagger\dagger}{=} -\frac{\bar{\lambda}\mathcal{V}_x(t,x,v)}{x\mathcal{V}_{xx}(t,x,v)} - \frac{\sigma\rho\mathcal{V}_{xv}(t,x,v)}{x\mathcal{V}_{xx}(t,x,v)} \\
&=: \pi^*(t,x,v) \\
&\overset{\dagger\dagger\dagger}{>} 0,
\end{aligned}$$

where † follows from dividing through by xv, †† was simply undwinding the shorthand notation and † † † from the assumption $\mathcal{V}_{xx} < 0$. Lastly, we have:

$$\begin{aligned}
g''(\pi) &= x\mathcal{V}_{xx} \\
&\overset{\dagger}{<} 0.
\end{aligned}$$

where † follows from $\mathcal{V}_{xx} < 0$ and $x > 0$. It is thus shown that equation (23), π^*, is a unique maximizer to $g(\pi)$.

⋆ By substitution of equation (23) into equation (22) with trial by fire and algebra now yields the PDE in $\mathcal{V}$ with terminal condition $\mathcal{V}(T,x,v)=U(x)$:

$$
\begin{aligned}
0 &= \mathcal{V}_t + \frac{1}{2}\sigma^2 v\mathcal{V}_{vv} + \kappa(\theta - v)\mathcal{V}_v + \sup_{\pi}\left\{x\left(r+\pi\bar{\lambda}v\right)\mathcal{V}_x + \frac{1}{2}\pi^2x^2v\mathcal{V}_{xx} + \pi x\sigma v\rho\mathcal{V}_{xv}\right\} \\
&= \mathcal{V}_t + \frac{1}{2}\sigma^2 v\mathcal{V}_{vv} + \kappa(\theta - v)\mathcal{V}_v + x\left(r+\pi^*(t,x,v)\bar{\lambda}v\right)\mathcal{V}_x + \frac{1}{2}\left(\pi^*(t,x,v)\right)^2x^2v\mathcal{V}_{xx} + \pi^*(t,x,v)x\sigma v\rho\mathcal{V}_{xv} \\
&= \mathcal{V}_t + \frac{1}{2}\sigma^2 v\mathcal{V}_{vv} + \kappa\theta\mathcal{V}_v - \kappa v\mathcal{V}_v + xr\mathcal{V}_x + \pi^*(t,x,v)x\bar{\lambda}v\mathcal{V}_x + \frac{1}{2}\left(\pi^*(t,x,v)\right)^2x^2v\mathcal{V}_{xx} + \pi^*(t,x,v)x\sigma v\rho\mathcal{V}_{xv} \\
&= \mathcal{V}_t + \kappa\theta\mathcal{V}_v + xr\mathcal{V}_x + v\left(\frac{1}{2}\sigma^2\mathcal{V}_{vv} - \kappa\mathcal{V}_v + \pi^*(t,x,v)\left(x\bar{\lambda}\mathcal{V}_x + \frac{1}{2}\pi^*(t,x,v)x^2\mathcal{V}_{xx} + x\sigma\rho\mathcal{V}_{xv}\right)\right) \\
&= \mathcal{V}_t + \kappa\theta\mathcal{V}_v + xr\mathcal{V}_x + v\left(\frac{1}{2}\sigma^2\mathcal{V}_{vv} - \kappa\mathcal{V}_v + \left(-\bar{\lambda}\frac{\mathcal{V}_x}{x\mathcal{V}_{xx}} - \sigma\rho\frac{\mathcal{V}_{xv}}{x\mathcal{V}_{xx}}\right)\left(x\bar{\lambda}\mathcal{V}_x + \frac{1}{2}\left(-\bar{\lambda}\frac{\mathcal{V}_x}{x\mathcal{V}_{xx}} - \sigma\rho\frac{\mathcal{V}_{xv}}{x\mathcal{V}_{xx}}\right)x^2\mathcal{V}_{xx} + x\sigma\rho\mathcal{V}_{xv}\right)\right) \\
&= \mathcal{V}_t + \kappa\theta\mathcal{V}_v + xr\mathcal{V}_x + v\left(\frac{1}{2}\sigma^2\mathcal{V}_{vv} - \kappa\mathcal{V}_v + \left(-\bar{\lambda}\frac{\mathcal{V}_x}{x\mathcal{V}_{xx}} - \sigma\rho\frac{\mathcal{V}_{xv}}{x\mathcal{V}_{xx}}\right)\left(x\bar{\lambda}\mathcal{V}_x - \frac{1}{2}\bar{\lambda}\mathcal{V}_xx - \frac{1}{2}x\sigma\rho\mathcal{V}_{xv} + x\sigma\rho\mathcal{V}_{xv}\right)\right) \\
&= \mathcal{V}_t + \kappa\theta\mathcal{V}_v + xr\mathcal{V}_x + v\left(\frac{1}{2}\sigma^2\mathcal{V}_{vv} - \kappa\mathcal{V}_v + \frac{1}{\mathcal{V}_{xx}}\left(-\bar{\lambda}\mathcal{V}_x\frac{1}{x} - \sigma\rho\frac{1}{x}\mathcal{V}_{xv}\right)\left(\frac{1}{2}\bar{\lambda}\mathcal{V}_xx + \frac{1}{2}x\sigma\rho\mathcal{V}_{xv}\right)\right) \\
&= \mathcal{V}_t + \kappa\theta\mathcal{V}_v + xr\mathcal{V}_x + v\left(\frac{1}{2}\sigma^2\mathcal{V}_{vv} - \kappa\mathcal{V}_v + \frac{1}{\mathcal{V}_{xx}}\left(-\frac{1}{2}\left(\bar{\lambda}\mathcal{V}_x\right)^2 - \frac{1}{2}\sigma\rho\bar{\lambda}\mathcal{V}_x\mathcal{V}_{xv} - \frac{1}{2}\bar{\lambda}\sigma\rho\mathcal{V}_x\mathcal{V}_{xv} - \frac{1}{2}\left(\sigma\rho\mathcal{V}_{xv}\right)^2\right)\right) \\
&= \mathcal{V}_t + \kappa\theta\mathcal{V}_v + xr\mathcal{V}_x + v\left(\frac{1}{2}\sigma^2\mathcal{V}_{vv} - \kappa\mathcal{V}_v + \frac{1}{\mathcal{V}_{xx}}\left(-\frac{1}{2}\left(\bar{\lambda}\mathcal{V}_x\right)^2 - \sigma\rho\bar{\lambda}\mathcal{V}_x\mathcal{V}_{xv} - \frac{1}{2}\left(\sigma\rho\mathcal{V}_{xv}\right)^2\right)\right) \\
&= \mathcal{V}_t + \kappa\theta\mathcal{V}_v + xr\mathcal{V}_x + v\left(\frac{1}{2}\sigma^2\mathcal{V}_{vv} - \kappa\mathcal{V}_v - \frac{1}{2}\left(\bar{\lambda}\mathcal{V}_x + \sigma\rho\mathcal{V}_{xv}\right)^2\frac{1}{\mathcal{V}_{xx}}\right) \\
&= \mathcal{V}_t + \kappa\theta\mathcal{V}_v + xr\mathcal{V}_x + v\left(\frac{1}{2}\sigma^2\mathcal{V}_{vv} - \kappa\mathcal{V}_v - \frac{1}{2}\frac{\left(\bar{\lambda}\mathcal{V}_x + \sigma\rho\mathcal{V}_{xv}\right)^2}{\mathcal{V}_{xx}}\right),
\end{aligned}
$$

which is equation (24) as desired.

⋆ We recall the terminal condition is $\mathcal{V}(T,x,v)=U(x)=x^p/p$. The seperation guessed solution (ansatz) for the optimal solution is equation (25). Firstly, we find the respective derivatives of $\mathcal{V}$ from equation (25):

$$
\mathcal{V}_x = ph\frac{x^{p-1}}{p}, \quad \mathcal{V}_{xx} = (p-1)x^{p-2}h, \quad \mathcal{V}_{xv} = x^{p-1}h_v
$$

Substituting in the found derivatives into equation (23) now yields that the optimal investment strategy is given by:

$$
\begin{aligned}
\pi^*(t,x,v) &= -\frac{\bar{\lambda}\mathcal{V}_x}{x\mathcal{V}_{xx}} - \frac{\sigma\rho\mathcal{V}_{xv}}{x\mathcal{V}_{xx}} \\
&= -\frac{\bar{\lambda}x^{p-1}h}{x(p-1)x^{p-2}h} - \sigma\rho\frac{x^{p-1}h_v}{x(p-1)x^{p-2}h} \\
&= -\frac{\bar{\lambda}}{p-1} - \frac{\sigma\rho}{p-1}\frac{h_v}{h} \\
&= \frac{\bar{\lambda}}{1-p} + \frac{\sigma\rho}{1-p}\frac{h_v}{h},
\end{aligned}
$$

which is exactly equation (26).

⋆ Firstly, we find the respective derivatives of $\mathcal{V}$ from equation (25):

$$\mathcal{V}_t = \frac{x^p}{p}h_t, \qquad \mathcal{V}_x = ph\frac{x^{p-1}}{p} = x^{p-1}h, \qquad \mathcal{V}_{xx} = (p-1)x^{p-2}h,$$
$$\mathcal{V}_{xv} = x^{p-1}h_v, \qquad \mathcal{V}_v = \frac{x^p}{p}h_v, \qquad \mathcal{V}_{vv} = \frac{x^p}{p}h_{vv}.$$

Substituting the found derivatives into equation (24) yields the PDE for h:

$$\begin{aligned}
0 &= \mathcal{V}_t + \kappa\theta\mathcal{V}_v + xr\mathcal{V}_x + v\left(\frac{1}{2}\sigma^2\mathcal{V}_{vv} - \kappa\mathcal{V}_v - \frac{1}{2}\frac{\left(\bar{\lambda}\mathcal{V}_x + \sigma\rho\mathcal{V}_{xv}\right)^2}{\mathcal{V}_{xx}}\right) \\
&= \frac{x^p}{p}h_t + \kappa\theta\frac{x^p}{p}h_v + xrx^{p-1}h + v\left(\frac{1}{2}\sigma^2\frac{x^p}{p}h_{vv} - \kappa\frac{x^p}{p}h_v - \frac{1}{2}\frac{\left(\bar{\lambda}x^{p-1}h + \sigma\rho x^{p-1}h_v\right)^2}{(p-1)x^{p-2}h}\right) \\
&= \frac{x^p}{p}h_t + \kappa\theta\frac{x^p}{p}h_v + rx^ph + v\left(\frac{1}{2}\sigma^2\frac{x^p}{p}h_{vv} - \kappa\frac{x^p}{p}h_v - \frac{1}{2}\frac{x^{2p-2}\left(\bar{\lambda}h + \sigma\rho h_v\right)^2}{(p-1)x^{p-2}h}\right) \\
&= \frac{x^p}{p}h_t + \kappa\theta\frac{x^p}{p}h_v + rx^ph + v\left(\frac{1}{2}\sigma^2\frac{x^p}{p}h_{vv} - \kappa\frac{x^p}{p}h_v - \frac{1}{2}\frac{x^p\left(\bar{\lambda}h + \sigma\rho h_v\right)^2}{(p-1)h}\right) \\
&= \frac{x^p}{p}h_t + \kappa\theta\frac{x^p}{p}h_v + rx^ph + v\left(\frac{1}{2}\sigma^2\frac{x^p}{p}h_{vv} - \kappa\frac{x^p}{p}h_v + \frac{1}{2}\frac{x^p\left(\bar{\lambda}h + \sigma\rho h_v\right)^2}{(1-p)h}\right) \\
&= \frac{x^p}{p}\left(h_t + \kappa\theta h_v + prh + v\left(\frac{1}{2}\sigma^2h_{vv} - \kappa h_v + \frac{1}{2}\frac{p\left(h\bar{\lambda} + \rho\sigma h_v\right)^2}{(1-p)h}\right)\right) \\
&\iff \\
0 &= h_t + \kappa\theta h_v + prh + v\left(\frac{1}{2}\sigma^2h_{vv} - \kappa h_v + \frac{1}{2}\frac{p\left(h\bar{\lambda} + \rho\sigma h_v\right)^2}{(1-p)h}\right),
\end{aligned}$$

which is exactly equation (27).

⋆ Firstly, we find the derivatives of h given in equation (28):

$$\begin{aligned} h_t &= \left(a'(\tau)\cdot(-1) + vb'(\tau)\cdot(-1)\right)h = -a'(\tau)h - b'(\tau)h_v, \\ h_v &= b(\tau)h, \quad h_{vv} = b^2(\tau)h. \end{aligned}$$

Substituting the found derivatives into equation (27), rearranging the terms to emphasize the linearity in v as asked to, yields:

$$\begin{aligned} 0 &= h_t + \kappa\theta h_v + prh + v\left(\frac{1}{2}\sigma^2 h_{vv} - \kappa h_v + \frac{1}{2}\frac{p\left(\bar{\lambda}h + \sigma\rho h_v\right)^2}{(1-p)h}\right) \\ &= h_t + \kappa\theta h_v + prh + v\left(\frac{1}{2}\sigma^2 h_{vv} - \kappa h_v + \frac{p\bar{\lambda}^2 h^2}{2(1-p)h} + \frac{p\sigma^2\rho^2 h_v^2}{2(1-p)h} + \frac{2p\bar{\lambda}\sigma\rho h h_v}{2(1-p)h}\right) \\ &= h_t + \kappa\theta h_v + prh + v\left(\frac{1}{2}\sigma^2 h_{vv} - \kappa h_v + \frac{p\bar{\lambda}^2 h}{2(1-p)} + \frac{p\sigma^2\rho^2 h_v^2}{2(1-p)h} + \frac{p\bar{\lambda}\sigma\rho h_v}{1-p}\right) \\ &= -a'(\tau)h - b'(\tau)h_v + \kappa\theta b(\tau)h + prh + v\left(\frac{1}{2}\sigma^2 b^2(\tau)h - \kappa b(\tau)h + \frac{p\bar{\lambda}^2 h}{2(1-p)} + \frac{p\sigma^2\rho^2 b^2(\tau)h^2}{2(1-p)h} + \frac{p\bar{\lambda}\sigma\rho b(\tau)h}{1-p}\right) \\ &= -a'(\tau)h + b(\tau)\kappa\theta h + prh + v\left(-b'(\tau)h + b^2(\tau)\left(\frac{1}{2}\sigma^2 h + \frac{p\sigma^2\rho^2 h}{2(1-p)}\right) + b(\tau)\left(-\kappa h + \frac{p\bar{\lambda}\sigma\rho h}{1-p}\right) + \frac{p\bar{\lambda}^2 h}{2(1-p)}\right), \end{aligned}$$

exactly as we wanted to show.

⋆ The previously derived Partial Differential Equation (PDE) is satisfied if and only if both conditions $(***)$ and $(****)$ are equal to zero. This condition is necessary for the PDE to be valid for all $\tau > 0$. As a result, these conditions lead to a set of Ordinary Differential Equations (ODEs) derived from $(***)$ and $(****)$, which can be tackled independently (similar to our approach in Subsection 1.2). Eliminating the terms involving h and reorganizing the PDE, we deduce two separate ordinary differential equations concerning the functions a and b:

$$
\begin{aligned}
0 &= -a'(\tau)h + b(\tau)\kappa\theta h + prh \\
&\quad + v\left(-b'(\tau)h + b^2(\tau)\left(\frac{1}{2}\sigma^2 h + \frac{p\sigma^2\rho^2h^2}{2(1-p)}\right) + b(\tau)\left(-\kappa h + \frac{p\bar{\lambda}\sigma\rho h}{1-p}\right) + \frac{p\bar{\lambda}^2 h}{2(1-p)}\right) \\
&\iff \\
0 &= h\left(\underbrace{-a'(\tau) + b(\tau)\kappa\theta + pr}_{(***)}\right) \\
&\quad + vh\Bigg(\underbrace{-b'(\tau) + b^2(\tau)\left(\frac{1}{2}\sigma^2 + \frac{p\sigma^2\rho^2}{2(1-p)}\right) + b(\tau)\left(-\kappa + \frac{p\bar{\lambda}\sigma\rho}{1-p}\right) + \frac{p\bar{\lambda}^2}{2(1-p)}}_{(****)}\Bigg) \\
&\iff \\
&\begin{cases}
\underbrace{-a'(\tau) + b(\tau)\kappa\theta + pr}_{(***)} = 0, \\
\underbrace{-b'(\tau) + b^2(\tau)\left(\frac{1}{2}\sigma^2 + \frac{p\sigma^2\rho^2}{2(1-p)}\right) + b(\tau)\left(-\kappa + \frac{p\bar{\lambda}\sigma\rho}{1-p}\right) + \frac{p\bar{\lambda}^2}{2(1-p)}}_{(****)} = 0
\end{cases} \\
&\overset{\dagger}{\iff} \\
&\begin{cases}
a'(\tau) = \kappa\theta b(\tau) + pr, \\
b'(\tau) = \frac{1}{2}\underbrace{\left(\sigma^2 + \frac{p\sigma^2\rho^2}{1-p}\right)}_{=:k_2} b^2(\tau) - \underbrace{\left(\kappa - \frac{p\bar{\lambda}\sigma\rho}{1-p}\right)}_{=:k_1} b(\tau) + \frac{1}{2}\underbrace{\frac{p\bar{\lambda}^2}{1-p}}_{=:k_0}
\end{cases} \\
&\iff \\
&\begin{cases}
a'(\tau) = \kappa\theta b(\tau) + pr, \\
b'(\tau) = \frac{1}{2}k_2 b^2(\tau) - k_1 b(\tau) + \frac{1}{2}k_0,
\end{cases} \quad ,
\end{aligned}
$$

where the underbraces in † follow from the Handin #3 description. Furthermore, we are told that the boundary condition for h is exactly given by $h(T, z) = 1, \forall z > 0$, which yields:

$$
\begin{aligned}
h(T, z) &= \exp\left\{a(\tau(T)) + b(\tau(T))z\right\} \\
&= 1 \\
&\iff \\
a(0) = a(\tau(T)) = 0 \quad &\text{and} \quad b(0) = b(\tau(T)) = 0,
\end{aligned}
$$

which defines the sufficient boundary conditions for the functions a, b.

⋆ By equation (28) we can rewrite to:

$$\mathcal{V}_{xx} = (p-1)x^{p-2}\exp\{a(\tau)+b(\tau)v\}$$

Using the definitions for k_i (and not κ), $i \in \{0,1,2\}$ that are underbraced in the first equality in equation (30) now yields:

$$\begin{aligned}
k^2(1-k_0k_2) &= \left(\kappa - \frac{p\bar{\lambda}\sigma\rho h}{1-p}\right)^2 - \left(\frac{p\bar{\lambda}^2}{1-p}\right)\left(\sigma^2 + \frac{p\sigma^2\rho^2}{1-p}\right) \\
&= \kappa^2 + \frac{p^2\bar{\lambda}^2\sigma^2\rho^2}{(1-p)^2} - 2\kappa\frac{p\bar{\lambda}\sigma\rho}{1-p} - \frac{p\bar{\lambda}^2}{1-p}\sigma^2 - \frac{p^2\bar{\lambda}^2\sigma^2\rho^2}{(1-p)^2} \\
&= \kappa^2 - 2\kappa\frac{p\bar{\lambda}\sigma\rho}{1-p} - \frac{p\bar{\lambda}^2}{1-p}\sigma^2 \\
&= \kappa^2 - \frac{2\kappa p\bar{\lambda}\sigma\rho - p\bar{\lambda}^2}{1-p}\sigma^2 \\
&= \frac{\kappa^2(1-p) - 2\kappa p\bar{\lambda}\sigma\rho h - p\bar{\lambda}^2\sigma^2}{1-p} \\
&> 0 \\
&\iff \\
1-p &> 0 \\
&\Rightarrow \\
\mathcal{V}_{xx} &= (p-1)x^{p-2}\exp\{a(\tau)+b(\tau)v\} \\
&< 0,
\end{aligned}$$

where we used the fact that $p-1<0$ and then also $1-p>0$ remembering $p \in (-\infty,0)\cup(0,1)$. Using now the previously found derivative, $h_v = b(\tau)h$, of h means we can write equation (26) as:

$$\begin{aligned}
\pi^*(t,x,v) &= \frac{\bar{\lambda}}{1-p} + \frac{\sigma\rho}{1-p}\frac{h_v}{h} \\
&= \frac{\bar{\lambda}}{1-p} + \frac{\sigma\rho}{1-p}\frac{b(\tau)h}{h} \\
&= \frac{\bar{\lambda}}{1-p} + \frac{\sigma\rho}{1-p}b(\tau),
\end{aligned}$$

and thus conclude that the candidate for the optimal investment strategy is indeed given by equation (33) with $b(t)$ given by equation (32) and $\tau = T-t$ (such that $b(\tau(t))$, yielding:

$$\pi^*(t,x,v) = \frac{\bar{\lambda}}{1-p} + \frac{\sigma\rho}{1-p}b(\tau(t)).$$

3.3 Interpretation of the results

⋆ All the code can be viewed in Appendix A.

To perform a sensitivity analysis on the optimal investment strategy π^* in relation to the model parameters, π^* has been expressed as a function of time $t \in [0, T]$, utilizing equations (33) and (32). As such, we define a `optimalpi`-function defined as in the Handin #3 description. This representation enables the generation of plots for $\pi^*(t)$ from $t = 0$ to expiry-T.

Firstly, expiry is set to $T = 10$. We define t to ensure that there is a time point for each business day within the year, resulting in a vector $t = T - \tau$ that includes $252 \cdot 10$ time points.

Initially, we will determine the values of the optimal investment strategy π^* as a function of time using selected parameter values. This strategy will act as our benchmark. For the sensitivity analysis, we will examine the impact of altering each parameter on π^* over time and compare these effects against the benchmark. This analysis will involve creating a separate plot for each parameter, focusing on one parameter at a time.

The analysis in `Python`$\frac{1}{2}$ is done with the benchmark parameters seen in Table 10 with the sensitivity analysis utilizing varying degrees of the benchmark. When a varying parameter is scrutinize all others are held constant at their benchmark.

Description	**Symbol**	**Value**
Speed of Mean Reversion	κ	1
Volatility of the Volatility	σ	0.3
Correlation Coefficient	ρ	-0.5
Risk-Aversion Parameter	p	0.5
Risk Premium per Unit of Variance	$\bar{\lambda}$	0.4
Expiry Time	T	10

Table 10: Model parameters used for the sensitivity analysis of π^*.

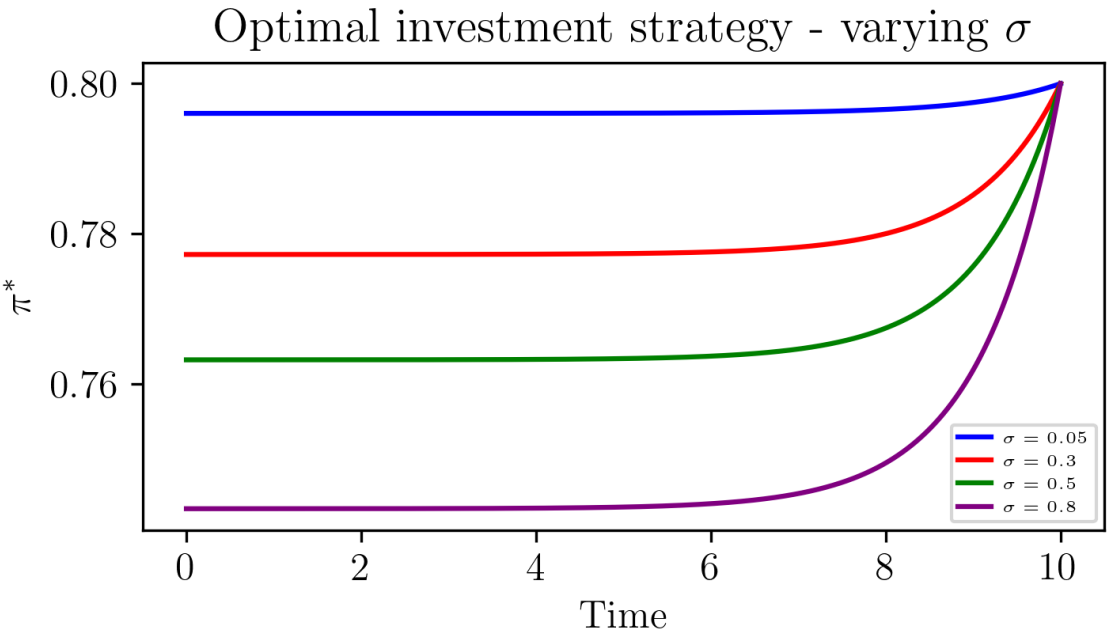

Figure 2: The optimal investing strategy for varying σ.

In Figure 2, the benchmark investment strategy is illustrated, where σ has been set to 0.3. Additionally, the Volatility of the Volatility (Vol-of-Vol) parameter σ is varied, and the optimal investment strategies for $\sigma \in \{0.05, 0.5, 0.8\}$ are computed, with all other parameters held constant.

At the expiry, all values of σ converge to an optimal investment strategy value of 0.8, indicating uniformity at this point. The graph shows that for the benchmark case 0.3, the optimal investment strategy increases gradually over time for the given parameters. As σ increases, the initial value of the optimal strategy decreases, which aligns with intuitive financial principles; higher σ typically leads to a more conservative investment stance as uncertainty arises at investment-time. The end-state uniformity across all values of σ implies that higher initial values result in a steeper curve as the strategy approaches the expiry, reflecting a more aggressive investment strategy over time. Conversely, when σ is very low, it becomes sensible to increase the optimal investments at $t = 0$ due to reduced uncertainty, suggesting that the optimal investment strategy remains quite stable in this scenario. This is entirely reasonable since σ represents the vol-of-vol, essentially quantifying the variability of the variance. As expected, π^* will fluctuate more with an increase in the vol-of-vol, where uncertainty is higher, and will be more consistent under conditions of low volatility.

Therefore, it is evident that σ does not influence the optimal investment level at expiry, but affects it in earlier periods untill nearing expiry-T.

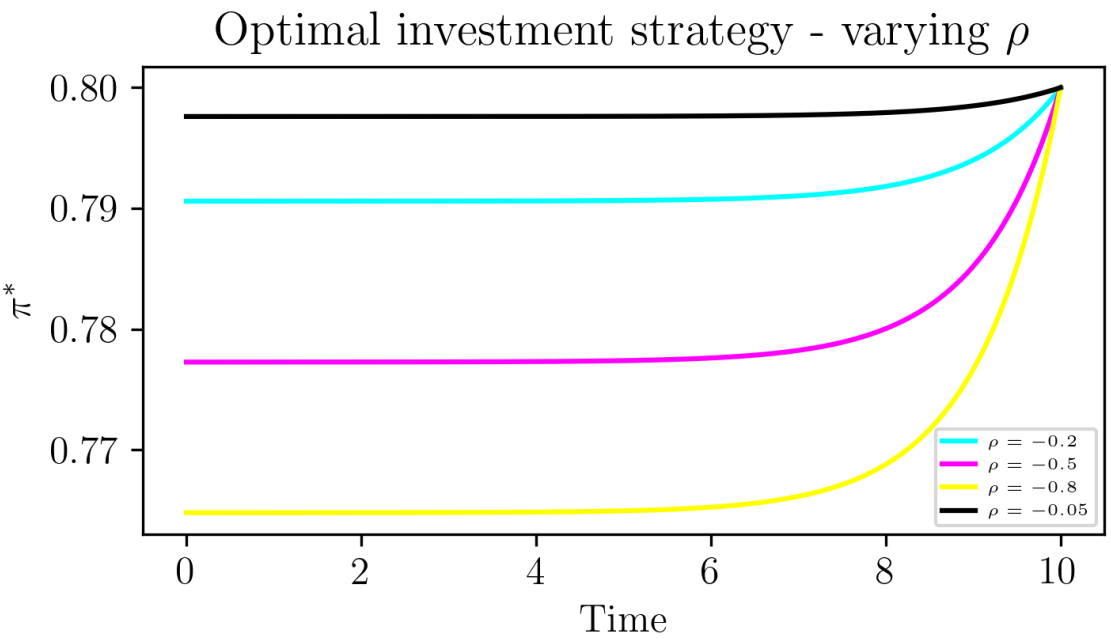

Figure 3: The optimal investing strategy for varying ρ.

In Figure 3, the benchmark investment strategy is illustrated, where ρ has been set to -0.5. Additionally, the Correlation Coefficient ρ is varied, and the optimal investment strategies for $\rho \in \{-0.05, -0.2, -0.8\}$ are computed, with all other parameters held constant. Note that from empirical observations of the financial markets $\rho < 0$.

As previously noted, we observe that at expiry, the optimal investment strategy π^* consistently attains a value of 0.8, independent of the chosen ρ. The variable ρ characterizes the correlation between two Brownian motions. Analysis of the plot indicates that a small numerical value of ρ leads to a higher initial investment. Furthermore, the value of the optimal investment strategy remains relatively stable over time. Conversely, when ρ is numerically larger, the enhanced negative correlation between the Brownian motions necessitates a lower initial optimal investment strategy. This scenario results in the optimal investment strategy gradually increasing over time, culminating uniformly at 0.8 by the expiry. This behavior is a consequence of the model dynamics.

The explanation hinges on understanding the relationship between the correlation coefficient, ρ, and the contributions of the two Brownian motions, W_1 and $W_2^{\mathbb{P}}$, to the dynamics of the asset price S_1 and its variance v. If ρ is numerically large, the contribution from $W_2^{\mathbb{P}}$ becomes negligible for movements in the variance, and thus it is only $W_1^{\mathbb{P}}$ that drives both dv and dS_1. This means that the optimal investment strategy is Initially low as there is a strong dependency between movements in both directions of the asset price and the variance, leading to a more cautious approach.

Conversely, if ρ is approximately zero, the contribution $W_1^{\mathbb{P}}$ to the variance is negligible and the variance is driven almost solely by $W_2^{\mathbb{P}}$, but the price is still driven by $W_1^{\mathbb{P}}$. A lower correlation $\rho \approx 0$ means that the relationship between S_1 and v is almost independent which allows for more aggressive investment strategies due to more predictable risk management. Furthermore, the lack of uncertainty allows for only minor corrections in investment near expiry. Conversely, a higher correlation (ρ numerically large) necessitates a more conservative approach due to increased perceived risk and uncertainty in the asset's price movements relative to its variance because of the

near independent relationsship between the risky asset S_1 and v.

In conclusion, ρ does not influence the ultimate level of the optimal investment strategy at expiry, but is affecting only the strategy in the earlier years.

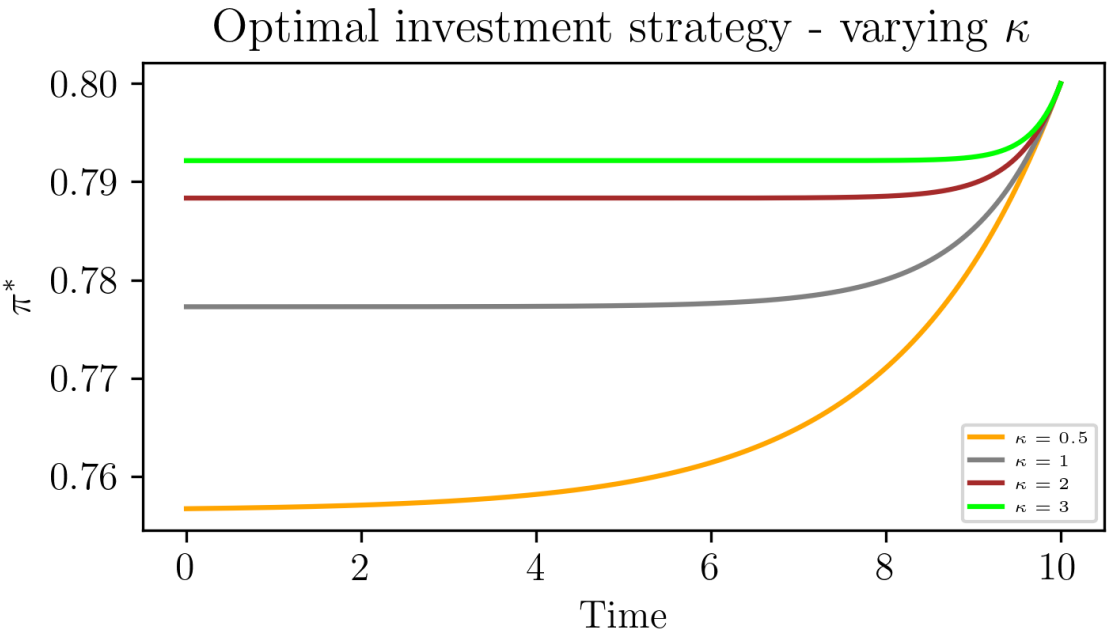

Figure 4: The optimal investing strategy for varying κ.

In Figure 4, the benchmark iznvestment strategy is illustrated, where κ has been set to 1. Additionally, the Mean Reversaion Rate κ is varied, and the optimal investment strategies for $\kappa \in \{0.5, 2, 3\}$ are computed, with all other parameters held constant.

It is clear that at expiration, the optimal investment strategy π^* is consistently 0.8, unaffected by the value of κ. The parameter κ denotes the mean reversion rate, reflecting how swiftly the variance of the asset returns to its long-term average, θ. According to the curves in Figure 4, a higher κ corresponds to an increased initial investment strategy. This makes sense because quicker mean reversion suggests a faster stabilization to the equilibrium state, allowing investors to predict future variances more confidently and adjust their portfolios aggressively in the short term with a higher optimal investment strategy.

On the other hand, a lower κ implies a longer duration for the variance to return to the mean, resulting in a more unpredictable variance process and thereby elevating the risk as uncertainty is more predominant until expiry. Consequently, a more conservative initial investment strategy is justified under these circumstances. Such conservative behavior mitigates the risk of exposure to high variance, thus safeguarding the investment against the potential for large fluctuations that could lead to substantial losses.

Therefore, while κ has no impact on the optimal investment level at expiration, it significantly influences the investment strategy during the initial years.

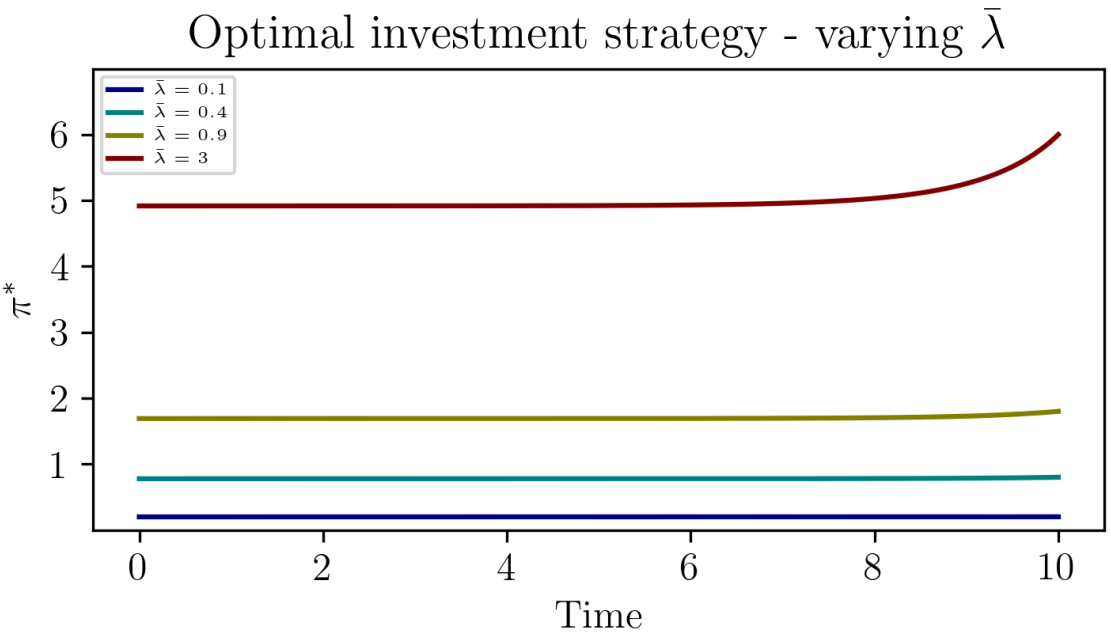

Figure 5: The optimal investing strategy for varying $\bar{\lambda}$.

In Figure 5, the benchmark investment strategy is illustrated, where $\bar{\lambda}$ has been set to 0.4. Additionally, the Risk Premium per Unit of Variance $\bar{\lambda}$ is varied, and the optimal investment strategies for $\bar{\lambda} \in \{0.1, 0.9, 3\}$ are computed, with all other parameters held constant. Note that from empirical observations of the financial markets $\bar{\lambda} > 0$.

Contrary to the earlier three plots, we now see that $\bar{\lambda}$ significantly influences the optimal investment strategy at expiry. $\bar{\lambda}$ serves as the indicator for volatility risk premium, providing insights into traders' risk tolerance and their decision-making aggressiveness. It is observed that a high $\bar{\lambda}$ correlates with an equally high optimal investment strategy. Essentially, a high $\bar{\lambda}$ suggests that the market compensates more for risk-taking, which in turn implies that investors are likely to invest more heavily and accept greater risks. According to Kraft (2005), there must be an upper limit to $\bar{\lambda}$; exceeding this limit would lead to excessively high market rewards for risk, rendering equations (31) and (32) invalid solutions for our model. This scenario leads to traders being overly optimistic about future gains, which logically results in observing elevated levels of optimal investment under high $\bar{\lambda}$. Additionally, a lower $\bar{\lambda}$ tends to stabilize the optimal investment strategy over time, unlike when $\bar{\lambda} = 3$, where the initial investment is significantly high and continues to rise at expiry, suggesting an overly generous market reward for risk.

Thus, while a higher $\bar{\lambda}$ generally encourages more aggressive investment strategies, reflecting a direct response to the higher rewards for risk-taking offered by the market, it is crucial to recognize the limits of this parameter. Adhering to realistic and sustainable investment practices requires careful calibration of $\bar{\lambda}$ within the models to ensure that the investment strategies formulated are both optimal and practical, aligning with genuine market dynamics and risk tolerance levels.

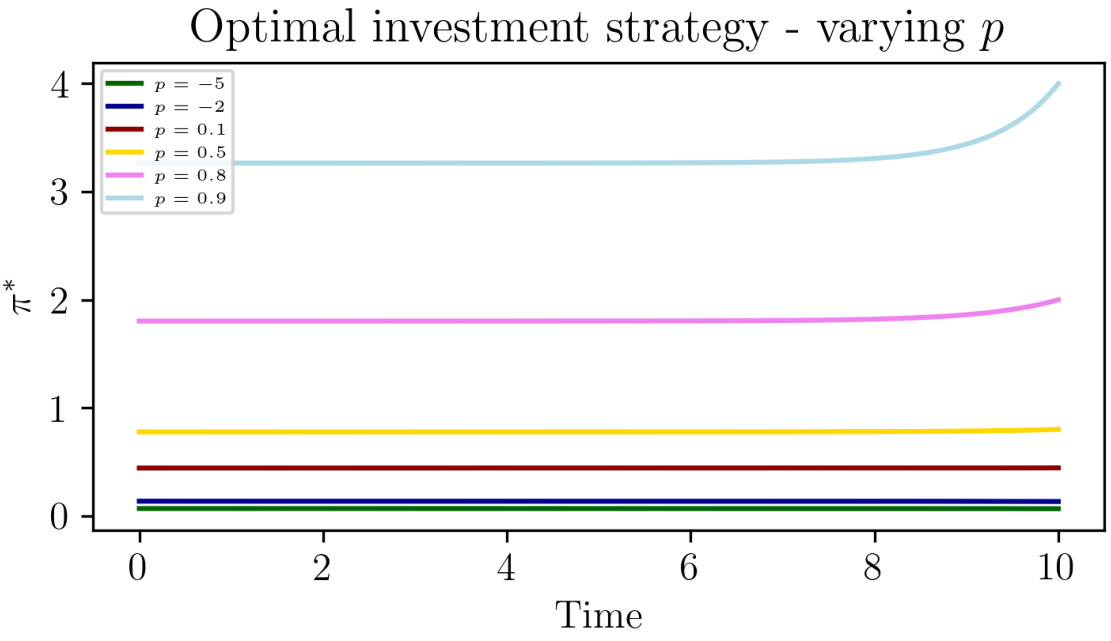

Figure 6: The optimal investing strategy for varying p.

In Figure 6, the benchmark investment strategy is illustrated, where p has been set to 0.5. Additionally, the Risk-Aversion Parameter p is varied, and the optimal investment strategies for $p \in \{-5, -2, 0.1, 0.8, 0.9\}$ are computed, with all other parameters held constant. Note $p \in (-\infty, 0) \cup (0, 1)$ by assumption.

Similar to $\bar{\lambda}$, we now find that p indeed impacts the optimal investment strategy at expiry and, consequently, over the long term. The plot reveals that when $p \in (-\infty, 0)$, the optimal investment level is quite low and remains consistently stable - or rather constant. Conversely, for $p \in (0, 1)$, the optimal investment strategy starts off low when p is near 0, but is still higher than when p is negative. As p approaches 1, the initial optimal investment strategy begins to increase. Notably, as p nears its upper limit ($p \approx 1$), the initial optimal investment strategy substantially increases, escalating further as we near expiry.

p represents the risk-aversion coefficient, indicating a trader's willingness to accept risk. When $p \in (0, 1)$, it characterizes a trader who is cautious yet open to taking risks, moving towards risk-neutrality as p nears 1. The plot confirms that with such traders, initial investments increase as perceived risks diminish or as potential returns appear more favorable. Specifically, we notice that at $p \approx 1$, optimal investment increases as expiry approaches. This correlates with decreased risk due to the shorter time to maturity, leading to more precise expectations. Additionally, this aligns well with the trader approaching risk-neutrality, allowing for slight variations in the optimal investment strategy over time, unlike the nearly constant strategy observed at lower p values. When $p \in (-\infty, 0)$, traders exhibit an even greater aversion to risk. This reflects precisely what the plot indicates: such traders maintain low and stable initial investments over time. In summary, as anticipated, traders more willing to accept risk ($p \in (0, 1)$) demonstrate more aggressive optimal investment behaviors as expiry approaches, optimizing their expected returns in line with their risk preferences. Conversely, traders who avoid risk ($p \in (-\infty, 0)$) exhibit low and stable optimal investment strategies.

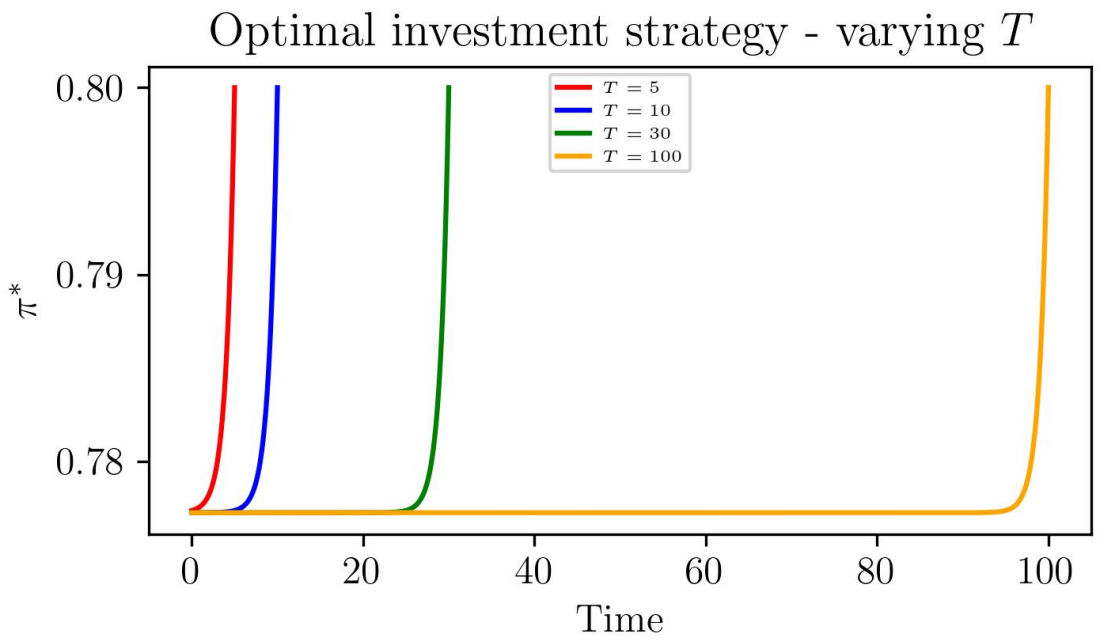

Figure 7: The optimal investing strategy for varying T.

In Figure 7, the benchmark investment strategy is illustrated, where T has been set to 10. Additionally, the Expiry Time T is varied, and the optimal investment strategies for $T \in \{5, 30, 100\}$ are computed, with all other parameters held constant.

We see that changing the expiry time T results in horizontal shifts for the curves, meaning, it has no effect on the optimal investment strategy in the interval $[0, T]$. This is as expected as - when all other parameters held constant - as the investment decision process does not inherently depend on the duration of the investment but rather on the underlying asset dynamics and the parameters controlling the investment strategy itself. Therefore, the expiry time T simply extends or shortens the investment horizon without altering the nature or direction of the investments within that period.

A Appendix: Code

GitHub profile with the code in `Python` for *Option Pricing in the Context of the Heston Model* and *Asset Allocation Under the Heston Model*. We frequently refer to and use the parameter "λ". It's crucial to understand that this "λ" parameter should not be confused with `Python`'s built-in `lambda`-function in subsection 2.3 and 2.4. `Python`'s `lambda` function is a feature that allows for creating small, anonymous functions at runtime. They are defined using the `lambda` keyword, followed by a list of arguments etc.

B References

H. Albrecher, P. A. Mayer, W. Schoutens, and J. Tistaert. The little heston trap. *Wilmott*, pages 83–92, January 2006.

T. Björk. *Arbitrage theory in continuous time*. Oxford university press, 4 edition, 2020.

Y. Havrylenko. Continuous-time finance 2: Stochastic volatility models and fourier methods in option pricing, week 8, 2024. `https://absalon.ku.dk/courses/72665/pages/week-8-april-2-4?module_item_id=2315776`.

S. L. Heston. A closed-form solution for options with stochastic volatility with applications to bond and currency options. *The review of financial studies*, 6(2):327–343, 1993.

H. Kraft. Optimal portfolios and heston's stochastic volatility model: an explicit solution for power utility. *Quantitative Finance*, 5(3):303–313, 2005.

F. D. Rouah. Euler and milstein discretization, 2024. `https://frouah.com/finance%20notes/Euler%20and%20Milstein%20Discretization.pdf`.

P. Virtanen, R. Gommers, T. E. Oliphant, M. Haberland, T. Reddy, D. Cournapeau, E. Burovski, P. Peterson, W. Weckesser, J. Bright, S. J. van der Walt, M. Brett, J. Wilson, K. J. Millman, N. Mayorov, A. R. J. Nelson, E. Jones, R. Kern, E. Larson, C. J. Carey, İ. Polat, Y. Feng, E. W. Moore, J. VanderPlas, D. Laxalde, J. Perktold, R. Cimrman, I. Henriksen, E. A. Quintero, C. R. Harris, A. M. Archibald, A. H. Ribeiro, F. Pedregosa, P. van Mulbregt, and SciPy 1.0 Contributors. SciPy 1.0: Fundamental Algorithms for Scientific Computing in Python. *Nature Methods*, 17:261–272, 2020. doi: 10.1038/s41592-019-0686-2.